

Long-lived central memory $\gamma\delta$ T cells confer protection against murine cytomegalovirus reinfection

Nathalie Yared¹, Maria Papadopoulou², Sonia Netzer¹, Laure Burguet¹, Lea Mora Charrot³, Benoit Rousseau³, Atika Zouine⁴, Xavier Gauthereau⁵, David Vermijlen², Julie Déchanet-Merville^{1*} and Myriam Capone^{1*}

* JDM and MC, co-senior authorship

¹ Bordeaux University, CNRS, ImmunoConcEpt, UMR 5164, 33076 Bordeaux, France.

² Department of Pharmacotherapy and Pharmaceutics and Institute for Medical Immunology, ULB Center for Research in Immunology (U-CRI), Université Libre de Bruxelles (ULB), Belgium.

³ Bordeaux University, Service Commun des Animaleries, 33076 Bordeaux, France

⁴ Bordeaux University, CNRS UAR3427, INSERM US05, FACSility, TBM Core, 33076 Bordeaux, France.

⁵ Bordeaux University, CNRS UAR3427, INSERM US05, OneCell, RT-PCR and Single Cell Libraries, TBM Core, 33076 Bordeaux, France.

Correspondence: CAPONE Myriam

UMR-CNRS 5164-ImmunoConCept, Bat 1B, 1er étage, Université de Bordeaux, 146 rue Leo Saignat, 33076 Bordeaux

Tel: 0033-5-57-57-95-74

Email: mcapone@immuconcept.org

Short title: $\gamma\delta$ T cell memory response to MCMV infection

ABSTRACT

The involvement of $\gamma\delta$ TCR-bearing lymphocytes in immunological memory has gained increasing interest due to their functional duality between adaptive and innate immunity. $\gamma\delta$ T effector memory (TEM) and central memory (TCM) subsets have been identified, but their respective roles in memory responses are poorly understood. In the present study, we used subsequent mouse cytomegalovirus (MCMV) infections of $\alpha\beta$ T cell deficient mice in order to analyze the memory potential of $\gamma\delta$ T cells. As for CMV-specific $\alpha\beta$ T cells, MCMV induced the accumulation of cytolytic, KLRG1+CX3CR1+ $\gamma\delta$ TEM that principally localized in infected organ vasculature. Typifying T cell memory, $\gamma\delta$ T cell expansion/proliferation in organs and blood was higher and more efficient after secondary viral challenge than after primary infection. Viral control upon MCMV reinfection involved the T-cell receptor, and was associated with a preferential amplification of private and unfocused TCR δ chain repertoire as evidenced by next generation sequencing. The $\gamma\delta$ T cell secondary response to MCMV was composed by a combination of clonotypes expanded post-primary infection and, more unexpectedly, of novel expanded clonotypes. Finally, Long-term-primed $\gamma\delta$ TCM cells, but not $\gamma\delta$ TEM cells, protected T cell-deficient hosts against MCMV-induced death upon adoptive transfer, probably through their ability to survive and to generate TEM in the recipient host. Overall, our study uncovered memory properties of long-lived TCM $\gamma\delta$ T cells that confer protection in a chronic infection, highlighting the interest of this T cell subset in vaccination approaches.

AUTHOR SUMMARY

Cytomegalovirus (CMV) is a widespread, latent virus that can cause severe organ disease in immune-compromised patients. Anti-CMV memory immune responses are essential to control viral reactivation and/or reinfection events that commonly take place in solid organ transplantation. The role of $\gamma\delta$ T-cell receptor bearing lymphocytes could be crucial in this context where immunosuppressive/ablative treatments cause suboptimal and/or delayed $\alpha\beta$ T cell responses. Here we asked whether $\gamma\delta$ T cells could compensate for the absence of $\alpha\beta$ T cells in the long-term control of mouse CMV infection. Three months post-primary viral challenge in $\alpha\beta$ -T cell deficient mice, $\gamma\delta$ T cells displayed similar features as cytolytic, CMV-specific $\alpha\beta$ CD8 T cells. We showed that previous priming with CMV endowed $\gamma\delta$ T cells with an enhanced antiviral potential and that long-term maintenance of $\gamma\delta$ -mediated antiviral protection was dependent on $\gamma\delta$ central memory T cells (TCM). The $\gamma\delta$ T cell response to a secondary CMV challenge was dependent on $\gamma\delta$ TCR-signaling and generated a private TCR δ repertoire as observed in human. Our results sustain the adaptive-like properties of these unconventional T cells and reveal the interest of targeting $\gamma\delta$ TCM subset in novel antiviral vaccination approaches.

INTRODUCTION

The concept of immunological memory has been challenged in recent years. It was described as an acquired, multidimensional and evolutionary process that can no longer be solely related to vertebrates and adaptive immunity. With regards to the host capacity to improve survival upon secondary infection, immunological memory implicates both the innate and adaptive arm of the immune system (reviewed in [1-3]).

Prototypical adaptive memory cells are CD8⁺ αβ T lymphocytes, composed of various populations harboring distinct migratory, proliferative and effector properties: CCR7⁺CD62L⁺CD27⁺ Central Memory T cells (TCM), mostly found in secondary lymphoid organs, and CCR7⁻CD62L⁻CD27⁻ Effector Memory T cells (TEM), among which CX3CR1⁺ circulating TEM and CX3CR1⁻CD103⁺CD49a⁺CD69⁺ Tissue-Resident Memory T cells (TRM). In the case of resolving infections, CD8 TEM progressively decline unless submitted to antigenic re-challenge. When the pathogen persists, these cells are retained and acquire specific features reminiscent to the nature of infection. In chronic infections (LCMV clone 13 in mice or HIV, HCV in humans), antiviral CD8 TEM display an increased expression of inhibitory receptors such as PD-1. In latent infections however (herpesviruses), such “exhausted” phenotype is uncommonly found, at least among circulating CD8 TEM (For reviews see [4-7]).

Among latent β-herpesviruses, cytomegaloviruses (CMVs) have drawn great attention due to the deleterious effects of CMV infection in immune-compromised individuals. In healthy subjects, remodeling of the CD8⁺ αβ TCR repertoire occurs over time during latency, with an increased frequency of cells specific for a few viral epitopes, a phenomenon referred to as memory inflation. Long-term CMV-induced CD8 T cells express a TEM KLRG1⁺ phenotype. In humans, they use the longer CD45 isoform (CD45RA), reminiscent of highly differentiated

cells. Inflationary CD8⁺ $\alpha\beta$ T cells circulate in the blood, home to peripheral tissues and show increased expression of cytolytic proteins. They are assumed to maintain robust function and prevent viral spread upon reactivation (for review see [8-11]). The crucial role of long-lasting memory to human CMV (HCMV) is exemplified in solid organ transplantation (SOT), where seronegative recipients (R-) receiving a CMV⁺ graft (D+) are at higher risk of developing CMV disease than seropositive recipients (R+).

Another population expressing somatically diversified, T-cell antigen (Ag) receptors (TCR) is delineated by MHC-unrestricted, $\gamma\delta$ TCR-bearing lymphocytes, which recognize ubiquitous stress-induced self ligands [12]. Their implication in immunological memory has been put forward in recent years, in different settings including pathogen infection and autoimmunity (reviewed [13-15]). Because of their dual nature, $\gamma\delta$ TCR-mediated memory responses display both innate-like and adaptive-like characteristics [16-18]. In fact, $\gamma\delta$ T cells are composed of so-called innate-like subsets with invariant and public (shared between individuals) TCR repertoires, as well as adaptive-like subsets with unfocused and highly private TCR repertoires. Innate-like $\gamma\delta$ T lymphocytes are preprogrammed before birth and thus display rapid effector function in periphery. On the other hand, adaptive-like $\gamma\delta$ T cells (which comprise mouse V γ 1⁺ and V γ 4⁺ and human non-V γ 9V δ 2 T cell subsets) exit the thymus after birth with a naïve phenotype. Reviewed in [19-21].

Some years ago, our group identified HCMV as a major driver of non-V γ 9V δ 2 clonal expansions in peripheral blood of renal transplant recipients, that was further on confirmed by other teams in different settings including allo-hematopoietic stem cell transplantation (HSCT) [22] (reviewed in [23, 24]). A $\gamma\delta$ T cell contribution to the anti-viral response was suggested by the concomitant diminution of viremia [25, 26]. The protective role of $\gamma\delta$ T cells was evidenced thanks to the mouse model. Concomitantly to the group of Winkler, we showed that $\gamma\delta$ T cells

can compensate for the absence of $\alpha\beta$ T cells and confer protection to mouse CMV (MCMV) (in $\text{TCR}\alpha^{-/-}$ or CD4-depleted $\text{CD8}^{-/-}$ JHT mice)[27, 28]. In $\text{TCR}\alpha^{-/-}$ mice, the acute phase response to MCMV engaged $\text{V}\gamma 1+$ and $\text{V}\gamma 4+$ T cells that acquired a $\text{CD44}^+\text{CD62L}^-$ (TEM) phenotype alongside infection resolution. To which extent and for how long previous contact with CMV endows $\gamma\delta$ T cells with an increased antiviral reactivity remains to be clarified.

As observed for HCMV-specific inflationary CD8^+ $\alpha\beta$ T lymphocytes, long-term HCMV-induced non- $\text{V}\gamma 9\text{V}\delta 2$ T cells express a TEMRA ($\text{CD45RA}^+\text{CD27}^-\text{CD62L}^-\text{CCR7}^-$) KLRG1^+ phenotype. Moreover, transplant patients experiencing a secondary infection (D-R+, *i.e.* HCMV-seropositive recipients receiving graft from a HCMV-seronegative donor) show a faster recall response of TEMRA $\gamma\delta$ T cells and better infection resolution comparatively to patients experiencing a primary infection (D+R-) [26, 29]. These results strongly suggest that $\gamma\delta$ T cells have a memory potential against CMV. In this study, we addressed this issue using our previously set up $\text{TCR}\alpha^{-/-}$ mouse model that allows experimental re-infection and adoptive transfer experiments. Our results show the preferential amplification of private TRD (TCR δ chain) repertoire upon MCMV reinfection, and highlight the crucial role of $\text{CD44}^+\text{CD62L}^-$ $\gamma\delta$ TCM for long-term maintenance of $\gamma\delta$ -mediated antiviral protection.

RESULTS

1. $\gamma\delta$ T cell response to secondary MCMV challenge is faster, higher and more efficient than during primary infection.

To test whether $\gamma\delta$ T cells have a memory potential against MCMV, we used subsequent infections of $\alpha\beta$ T cell deficient mice, which allowed direct demonstration of the protective

antiviral function of $\gamma\delta$ T cells [27]. Three months after a first contact with MCMV (*i.e.* time delay required for latency in wild type mice), TCR $\alpha^{-/-}$ mice were re-challenged with similar doses of MCMV, and the secondary $\gamma\delta$ T cell response was analyzed in the liver and lung. Age-matched control mice were primarily infected concomitantly (Fig 1A). When looking at $\gamma\delta$ T cell numbers, a more rapid and higher increase of $\gamma\delta$ T lymphocytes was observed after re-infection when compared to primary infection (Fig 1B, upper panels). The highest count was obtained at day 1 (d1) for liver and d7 for lung in re-infected mice, comparatively to d7 for liver and d14 for lung during primary infection. Concerning viral loads, DNA copies of MCMV were still detected in organs from d92-infected TCR $\alpha^{-/-}$ mice (Fig 1B, lower panels). However, after re-infection, they remained stable and even slightly decreased by contrast to the increase observed during primary infection.

In order to converge to analyses done in humans, we monitored the kinetic of $\gamma\delta$ T lymphocytes longitudinally, in blood samples from TCR $\alpha^{-/-}$ mice taken post primary and secondary MCMV-infection. In accord with previous findings, the first phase of infection was marked by a drop in $\gamma\delta$ T cell numbers, likely related to virus-driven lymphopenia (Fig 1C) [28, 30]). Then, $\gamma\delta$ T cell counts increased back to normal levels, reaching a peak at day 21. Interestingly, maximal numbers of $\gamma\delta$ T cells were obtained at day 7 post-reinfection, *i.e.* much earlier than after primary MCMV encounter.

Collectively, our data depict a more rapid and more efficient $\gamma\delta$ T cell response to MCMV after secondary challenge compared to the primary response, which are typical of T cell memory.

2. *KLRG1+* $\gamma\delta$ TEM dominate the $\gamma\delta$ T cell secondary response to MCMV

To characterize the memory $\gamma\delta$ T cell subsets involved in the recall response to MCMV, we followed the kinetic of $\gamma\delta$ T naïve (CD44 $^{-}$), TCM (CD44 $^{+}$ CD62L $^{+}$) and TEM (CD44 $^{+}$ CD62L $^{-}$)

) along the course of the experiment depicted in Fig 1A. Due to the broad antigen specificity of $\gamma\delta$ T cells and the presence of innate-like $\gamma\delta$ T cells in organs [31], an important proportion of $\gamma\delta$ TEM but few naïve $\gamma\delta$ T cells were evidenced in control uninfected mice (d0, S1A Fig). From d0 to d92, $\gamma\delta$ TEM percentages increased concomitantly to a decrease of TCM. Notably (Fig 2A), $\gamma\delta$ TEM numbers tripled up after secondary infection in organs (d7 for lung and d1 for liver), and blood (d7). Thus, the kinetic response of TEM in organs and blood (Fig 2A) followed that of total $\gamma\delta$ T cells (Fig 1B, upper panels and Fig 1C), once again typifying T cell memory.

Then, we assessed the presence of KLRG1 on $\gamma\delta$ TEM, based on the reported expression of this receptor on inflationary CMV-specific CD8⁺ $\alpha\beta$ T cells [32, 33]. The percentage of KLRG1⁺ among $\gamma\delta$ TEM importantly increased from d0 to d92 in MCMV-target organs and blood (S1B Fig). As depicted in Fig 2B (upper panels), the $\gamma\delta$ T cell secondary response was dominated by KLRG1⁺ $\gamma\delta$ TEM in the lung, while both KLRG1⁻ and KLRG1⁺ $\gamma\delta$ TEM subsets increased in the liver. Interestingly, the kinetic evolution of KLRG1⁺ $\gamma\delta$ T cell numbers in blood (Fig 2B, lower panels) resembled that of lung (Fig 2B, upper left), suggesting possible involvement of circulating $\gamma\delta$ TEM KLRG1⁺ cells in the pulmonary $\gamma\delta$ T cell response to MCMV.

3. MCMV leaves a long-lasting imprint on $\gamma\delta$ T cells

To understand how previous contact with MCMV shapes $\gamma\delta$ T lymphocytes in the long-term towards increased antiviral activity, we first conducted a comparative phenotypic analysis of $\gamma\delta$ T cells from three months infected *versus* uninfected TCR $\alpha^{-/-}$ mice. As shown in S2A Fig, KLRG1 and CX3CR1 were co-expressed on $\gamma\delta$ TEM, while KLRG1 and PD1 showed mutually exclusive expression (S2B Fig). The CX3CR1 receptor, which binds to the endothelial homing chemokine fractalkine, was previously found on the cell surface of V δ 1⁺ T lymphocytes induced by HCMV infection [34, 35]. In samples from MCMV-naïve mice, the majority of $\gamma\delta$ TEM were KLRG1-CX3CR1⁻ (Fig 3A, upper panels), akin to $\gamma\delta$ TCM (lower panels).

However, whereas $\gamma\delta$ TCM remained mostly KLRG1-CX3CR1⁻ in d92 infected mice, the proportion of KLRG1+CX3CR1⁺ cells among $\gamma\delta$ TEM markedly rose upon infection, especially in blood (Fig 3A). Intracellular analysis of granzyme A further showed that KLRG1+CX3CR1⁺ $\gamma\delta$ TEM from target organs of long-term infected mice exhibit higher cytolytic potential, comparatively to age-matched control mice (Fig 3B).

We next performed a multiplex gene expression analysis of immunology factors and receptors expressed by $\gamma\delta$ T cells purified from organs of uninfected and MCMV-infected mice (S3 Fig). Among the transcripts that were increased concomitantly in the liver and lung at d92 (S3A Fig), there were genes associated with cytotoxicity (*Gzma*, *Gzmb*, *Prfl*), inhibitory receptors (*Klrc*), as well as *Cx3cr1*. Evolution of these factors further showed their tendency to increase after reinfection (d7), especially in the lung (S3B Fig). In contrast, we evidenced a decrease of *Ccr7* and *Cdkn1a* (cyclin dependent kinase inhibitor 1) in long-term induced $\gamma\delta$ T cells from liver and lung (Fig S3A Fig).

Taken together, these results demonstrate that, as observed for $\alpha\beta$ T cells, MCMV leaves a long-lasting imprint on $\gamma\delta$ T cell phenotype and function, characterized by a raise of cytotoxic KLRG1+CX3CR1⁺ cells among $\gamma\delta$ TEM in target organs and blood.

4. Long-term $\gamma\delta$ TEM expressing KLRG1/CX3CR1 preferentially localize in organ vasculature

To gain a better knowledge on the localization of these long-term effector $\gamma\delta$ T cells likely involved in the local/tissue antiviral control, we discriminated vascular *versus* parenchyma $\gamma\delta$ T cell memory subsets, using anti-CD45 intravascular injection. The majority of $\gamma\delta$ T cells from the lung and liver of d92 infected mice appeared to be CD45⁺, thus positioned close to the vasculature (IV⁺) (Fig 4A). This repartition was not a consequence of infection since similar

results were obtained in control mice. Interestingly, $\gamma\delta$ TCM from infected lung were mostly found in the IV+ fraction, suggesting that these cells could be recruited to tissues from lymph nodes through blood flow (Fig 4B). CX3CR1+KLRG1+ $\gamma\delta$ TEM were also largely enriched in the IV+ fraction (Fig 4C and 4D), in accord with preferential expression of CX3CR1 on peripheral memory T cells (TPM) [36]. Pulmonary “resident” $\gamma\delta$ TEM cells were indeed mainly composed of CX3CR1-KLRG1- cells expressing PD1 (Fig 4D). When comparing infected and uninfected mice, our results reveal a tendency toward higher CX3CR1+KLRG1+ and lower CX3CR1-KLRG1-PD1+ $\gamma\delta$ TEM in both IV+ and IV- cells from liver and lung.

Thus, long-term local/tissue $\gamma\delta$ T cell response to MCMV infection probably involves cells in both vascular and parenchyma compartments, but the most prevalent subset (i.e. $\gamma\delta$ TEM co-expressing KLRG1 and CX3CR1) preferentially localize in the vasculature.

5. Temporally Blocking $\gamma\delta$ TCM egress from lymph nodes poorly affects viral load control in organs from long-term infected mice

Our next goal was to determine whether blocking lymph nodes egress of TCM would affect the long-term $\gamma\delta$ T cell response to MCMV. To do so, we used fingolimod (FTY720) and analysed the consequence of short-term (11 days) treatment on $\gamma\delta$ TCM/TEM numbers and viral control. An important decrease of $\gamma\delta$ TCM counts was evidenced in blood, lung and liver when comparing untreated and FTY720-treated TCR $\alpha^{-/-}$ mice (Fig 5A, upper panels). In contrast, $\gamma\delta$ TEM numbers remained constant in organs from treated mice, although they were reduced in blood (Fig 5A, lower panel). FTY720-treatment poorly affected blood poorly affected the control of viral loads in long-term infected TCR $\alpha^{-/-}$ mice, since no statistical differences were evidenced in organs from control *versus* FTY720-treated mice (Fig 5B).

These results suggest that long-term $\gamma\delta$ T cell response to MCMV involves tissue control of viral loads by local $\gamma\delta$ TEM.

6. Viral control after reinfection engages $\gamma\delta$ -TCR signaling

To test whether the memory antiviral potential of $\gamma\delta$ T lymphocytes was dependent on TCR signaling, we used the anti- $\gamma\delta$ TCR mAb clone GL3, which induces down regulation of the surface expression of the TCR, rendering $\gamma\delta$ T cells invisible and poor responders to TCR-specific stimulation [37]. Three months post primary MCMV infection, TCR $\alpha^{-/-}$ mice received intravenous injection of GL3 or isotypic control mAb, followed (24h later) by MCMV secondary challenge (Fig 6A). The effect of the anti- $\gamma\delta$ TCR mAb treatment was confirmed by an absence of TCR δ surface expression (Fig 6B). Seven days post-re-infection, a substantial increase of viral loads was observed in organs from mice that had received the anti- $\gamma\delta$ TCR mAb comparatively to control mice (Fig 6C) indicating TCR involvement in $\gamma\delta$ T cell control of CMV.

7. MCMV drives the expansion of a private and adaptive-like TCR δ repertoire

As the $\gamma\delta$ TCR is involved in the viral control by long-term-induced $\gamma\delta$ T cells in our model, we tested whether there were changes in the TRD (TCR δ chain) repertoire upon MCMV infection. We performed TRD CDR3 NGS analysis on blood at different time points post-primary (short-term (d21), long-term (d80)) and post-secondary (d7R) MCMV infection. At d7R, the TRD repertoires of lung, liver and spleen were analyzed in parallel. Age-matched control mice were studied simultaneously to take into account possible impact of ageing [38]. No major differences were observed between uninfected (n=3) and infected mice (n=5) in TRDV usage, CDR3 length distribution and number of N additions (S4A Fig).

While the TRD repertoire appeared to be relatively stable between d21 and d80, important changes were observed after infection (d21) and reinfection (d7R) (Fig 7A, upper panels). Some clonotypes present at d0 (dark blue, mice 1 and 2) were barely found at d21, leaving space to other clonotypes (see for example mouse 1, where clone CALMEREAFWGGELSATDKLVF (TRDV2-2) became highly prominent). The secondary $\gamma\delta$ T cell response to MCMV was composed by a combination of clonotypes expanded post-primary infection and, more unexpectedly, of novel expanded clonotypes (for example mouse 2 and 3, Fig 7A in orange). Note that at d7R a higher TRD blood repertoire overlap with organs was observed compared to d0 (S5 Fig), indicating that the blood $\gamma\delta$ T cell response to MCMV reflects (at least partially) what occurs in organs at a given time point.

In comparison to infected mice, the kinetic evolution of clonotypes in blood of uninfected mice remained more stable overall, although some changes also occurred consecutively to control medium injection (Fig 7A, lower panels). Notably however, the frequency of shared clonotypes between individuals of the infected mice group (i.e. F value, a repertoire overlap measure) was lower than that of the control group (Fig 7B), while no clear influence could be observed on the diversity of the repertoire (S4B Fig), indicating that the TRD repertoire became more private upon MCMV infection (unique to each individual). Among the public sequences highly shared between samples, we identified the innate CDR3 amino acid sequences CGSDIGGSSWDTRQMFF (*TRDV4* sequence) [39-42] and CALWEPHIGGIRATDKLVF (TRAV15-1-DV6-1 sequence) related to so-called NK T $\gamma\delta$ [43, 44] (for nomenclature see [45]). In line with an increased private repertoire upon infection, a tendency towards lower representation of these shared clonotypes in infected *versus* uninfected mice was observed (Fig 7C).

In sum, our results highlight the preferential amplification and/or recruitment of a private and adaptive-like TRD repertoire upon MCMV infection. The $\gamma\delta$ T cell secondary response to

MCMV appears to involve both $\gamma\delta$ TCR clonotypes expanded after the primary MCMV encounter as well as novel expanded clonotypes.

8. Long-term MCMV-induced $\gamma\delta$ T cells confer protection to T cell deficient hosts upon adoptive transfer

To confirm the protective antiviral function of long-term induced $\gamma\delta$ T cells, $\gamma\delta$ T cells were isolated from the spleen of three month-MCMV-infected TCR $\alpha^{-/-}$ infected mice, and transferred into CD3 $\epsilon^{-/-}$ hosts (Fig 8A). $\gamma\delta$ T cells isolated from MCMV-infected mice importantly increased the survival rate of CD3 $\epsilon^{-/-}$ hosts that are infected with MCMV one day after the transfer (Fig 8B, left). Improved viral control in $\gamma\delta$ -T cell bearing versus T-cell deficient mice was evidenced by lower viral loads in organs (Fig 8B, right). In a second set of experiments, $\gamma\delta$ -T cells were sorted from age-matched control mice (5 months old) and transferred into T-cell deficient hosts. A control group of mice received $\gamma\delta$ T cells from d92 MCMV-infected mice as in the first experiment. CD3 $\epsilon^{-/-}$ hosts bearing “naïve” $\gamma\delta$ T cells (i.e. unprimed by MCMV) became moribund within same time-delay as T cell deficient hosts and bared comparable viral loads at sacrifice, in contrast to CD3 $\epsilon^{-/-}$ bearing MCMV-primed $\gamma\delta$ T cells (Fig 8C, upper panel). Higher quantities of transaminases were found in age-matched naïve $\gamma\delta$ -T cell bearing mice, comparatively to CD3 $\epsilon^{-/-}$ hosts that had received d92 MCMV-primed $\gamma\delta$ T cells (Fig 8C, lower left panel). Alongside, mice transferred with unprimed $\gamma\delta$ T lymphocytes had lower $\gamma\delta$ T cell counts (Fig 8C, lower right panel). Finally, we analyzed $\gamma\delta$ T cells in 5 CD3 $\epsilon^{-/-}$ mice that had survived for 130 days (i.e. transferred with d92 MCMV-primed $\gamma\delta$ T cells). The repartition of $\gamma\delta$ T cell memory subtypes in $\gamma\delta$ -bearing CD3 $\epsilon^{-/-}$ and d92 infected TCR $\alpha^{-/-}$ mice was comparable, evidencing efficient reconstitution (S6 Fig).

Thus, previous contact with MCMV endows $\gamma\delta$ T cells with an enhanced protective potential which may (at least partially) depend on a longer half-life in T-cell deficient hosts.

9. The protective function of d92 MCMV-induced $\gamma\delta$ T cells from the spleen principally relies on the presence of $\gamma\delta$ TCM

Long-lasting memory has long been attributed to $\alpha\beta$ TCM, while the function of $\gamma\delta$ TCM remains poorly studied. At day 92 post-MCMV infection, $\gamma\delta$ T cells from the spleen of $\text{TCR}\alpha^{-/-}$ mice comprised CD44⁺CD62L⁺ (TCM), CD44⁺CD62L⁻ (TEM) KLRG1⁺ (mostly CX3CR1⁺) and TEM KLRG1⁻ (mostly CX3CR1⁻) (S6 Fig on the top right). To gain knowledge on the protective function of these memory $\gamma\delta$ T cell subsets, we sorted $\gamma\delta$ TCM, TEM KLRG1⁺ and TEM KLRG1⁻ from the spleen of d92 MCMV-infected $\text{TCR}\alpha^{-/-}$ mice, and their protective function after transfer was assessed as above. Interestingly, $\gamma\delta$ TCM was the only subtype able to confer good protection to T-cell deficient hosts upon adoptive transfer (Fig 9A, upper panel). In moribund mice from the TEM KLRG1⁺ and KLRG1⁻ transfer groups, viral loads (Fig 9A, lower panels) and transaminase levels (Fig 9B) were elevated, with no statistical difference comparatively to the non-transferred group. In contrast, for both readouts, significant differences were observed between CD3 $\epsilon^{-/-}$ control mice and surviving mice from the TCM transfer group (Fig 9A, lower panels and fig 9B). Markedly, the majority of $\gamma\delta$ T cells recovered in $\gamma\delta$ TCM recipient mice display a CD44⁺CD62L⁻ TEM phenotype, and were for the most composed of KLRG1⁺CX3CR1⁺ cells in lung, and KLRG1⁻CX3CR1⁻ cells in the liver and spleen (Fig 9C). Finally, we showed that $\gamma\delta$ TCM from control and long-term MCMV-infected mice exhibit higher proliferative potential in culture with IL15, comparatively to $\gamma\delta$ TEM (S7 Fig).

These results univocally show that $\gamma\delta$ TCM are precursors of KLRG1⁺ and KLRG1⁻ $\gamma\delta$ TEM. Low numbers of MCMV-primed $\gamma\delta$ TCM are sufficient to maintain long-term antiviral activity against MCMV in T-cell deficient hosts, possibly through their capacity to survive and to generate $\gamma\delta$ TEM able to control viral loads in target organs.

DISCUSSION

In contrast to increasing numbers of studies showing the memory potential of $\gamma\delta$ T cells during acute resolving infections, data describing $\gamma\delta$ T cell memory in persistent infections are missing. CMV is the prototypical β -herpesvirus establishing lifelong latent infection. Anti-CMV memory responses are essential to control viral reactivation and/or reinfection events that commonly take place in SOT. The role of $\gamma\delta$ T cells could be significant in this context where immunosuppressive/ablative treatments cause suboptimal and/or delayed $\alpha\beta$ T cell responses [22]. In the present study, we used subsequent MCMV infections of TCR $\alpha^{-/-}$ mice to decipher the memory potential of $\gamma\delta$ T cells against CMV. Our data depict a more rapid and more efficient $\gamma\delta$ T cell secondary *versus* primary antiviral response in MCMV-target organs and blood, with the implication of $\gamma\delta$ TEM. They are in line with the faster increase of non-V γ 9V δ 2 TEMRA cells in blood from secondary infected HCMV-seropositive *versus* primary infected HCMV-seronegative renal transplant recipients, which associates to shorter infection resolution [26, 29]. Stressing the value of our mouse model, our study points out that $\gamma\delta$ T cell memory function can operate independently of priming with $\alpha\beta$ CD4 T cells. Furthermore, our adoptive transfer experiments show a major role for $\gamma\delta$ TCM in the maintenance of long-term antiviral activity.

Despite long-term survival of TCR $\alpha^{-/-}$ infected mice, DNA copies of MCMV were still detected in the liver and lung at d92. This suggests the continuous production of infectious virus in the absence of $\alpha\beta$ T cells. Even so, MCMV drove the accumulation of $\gamma\delta$ TEM that were mostly PD-1^{neg}, unlike T cells responding to chronic viruses such as non-cytopathic LCMV clone 13 [7]. In fact, $\gamma\delta$ TEM from d92-infected mice expressed KLRG1, a typical feature of CMV-induced $\alpha\beta$ CD8 TEM that was associated to antigen persistence rather than to viral replication [46, 47]. These results emphasize the importance of the intrinsic nature of pathogen in determining T cell fate, although the route and dose of infection may also operate [48, 49].

We show here mutually exclusive expression of KLRG1 and PD-1 on $\gamma\delta$ TEM, related to their anatomical localization. KLRG1+ $\gamma\delta$ TEM co-expressed CX3CR1 and were mainly located in the blood and intravascular compartment from organs, while PD-1+ $\gamma\delta$ TEM prevailed beyond the vasculature. Our results are in line with the recent study by Oxenius's team, who depicted a rise of pulmonary intravascular (IV+) KLRG1+ $\alpha\beta$ CD8 TEM driven by MCMV [50]. Interestingly, the increase of KLRG1+ $\gamma\delta$ TEM in the intravascular compartment occurred concomitantly to a decrease of KLRG1- $\gamma\delta$ T cells in the IV- fraction, suggesting a possible modulation of this receptor while $\gamma\delta$ T cells transit from the parenchyma to the blood circulation, and reciprocally. The accumulation of KLRG1+ $\gamma\delta$ TEM in long-term infected mice might thus reflect their continuous dissemination through the bloodstream in response to systemic MCMV infection.

Priming of $\gamma\delta$ T cells with MCMV induced transcription of genes associated to cytotoxicity, in accord with their reported capacity to kill CMV-infected fibroblasts, a function that could be important to control the virus *in vivo* [28]. In the liver, where the virus early disseminates *via* the intraperitoneal route, the fast mobilization of KLRG1- Granzyme A+ cells after secondary viral challenge sustains their implication in the control of local infection, possibly through

killing of MCMV-infected parenchymal cells (i.e. hepatocytes). Long-term MCMV-primed $\gamma\delta$ T cells also upregulated genes encoding NKR, including signaling lymphocyte activation molecules (SLAM). The latter are commonly found on cytotoxic effectors and may act as important rheostats to fine-tune their functions. The modulation of these transcripts along the course of MCMV infection and reinfection is reminiscent to repetitive antigen exposure [51], suggesting continuous triggering of the $\gamma\delta$ TCR by still-unknown MCMV-induced antigens. The concomitant downregulation of genes/protein involved in trafficking into lymph nodes suggest a preferential function of these cells in the tissues such as the liver and lung.

In spite of applying a second boost of MCMV, viral loads in organs remained mostly stable or even decreased after reinfection, although interindividual variations were noticed. Our results suggest that rapid virus handling upon MCMV secondary challenge might benefit from the long-lasting molecular imprint left on $\gamma\delta$ T cells by first MCMV encounter. This hypothesis is supported by the capacity of long-term MCMV-primed $\gamma\delta$ T cells to confer protection upon adoptive transfer into T-cell deficient hosts; in contrast, the time-delay needed to proliferate and differentiate probably precludes MCMV-naïve $\gamma\delta$ T cells to counteract the amplification and dissemination of viral copies. d92-induced $\gamma\delta$ T cells might have a higher survival rate, proliferative capacity, and/or effector function than unprimed $\gamma\delta$ T cells. Improved survivability of viral-primed $\gamma\delta$ T cells is suggested by the decline of transcripts encoding the cell-cycle inhibitor p21 (*Cdkn1a*), and by their maintenance upon transfer into T cell deficient hosts.

First evidence for $\gamma\delta$ T cell memory responses were put forward in the early 2000 and implicated phosphoantigen-reactive V γ 9V δ 2 in primates [52-54]. In mice, pioneering work was carried out by Lefrançois's team who showed higher increase of V γ 6V δ 1 cells in mesenteric lymph nodes after *Listeria monocytogenes* (*Lm*) secondary and even tertiary oral challenge, relatively to primary infection [55, 56]. Since then, increasing numbers of studies have shown the memory

potential of $\gamma\delta$ T cells in infections ([41, 42, 44] and reviewed in [13-15]). The $\gamma\delta$ T cell subtypes described in most of these studies are pre-activated lymphocytes with innate-like features and limited TCR diversity. In contrast, a tendency towards an increase in TRD diversity could be noticed in blood after MCMV reinfection, concomitant to a decrease of the highly frequent innate like CGSDIGGSSWDTRQMFF sequence, and to the acquisition of a more private TRD repertoire. Since innate-like $\gamma\delta$ T cells are commonly shared between mice, our results suggest the mobilization/amplification of private adaptive-like $\gamma\delta$ T cell clones soon after MCMV encounter. They are in line with our previous data showing, by the use of CD3 $\epsilon^{-/-}$ mice receiving TCR $\alpha^{-/-}$ bone marrow graft, that fetal-derived $\gamma\delta$ T cells are dispensable for long-term MCMV protection in the adult mice [27]. The participation of innate-like $\gamma\delta$ T cells in the antiviral response remains possible, and might be particularly relevant in humans where congenital HCMV infection can occur [34, 57]. Interestingly, expansion of private CDR3 β clones at the expense of more public ones was described by Friedman and colleagues following immunization with either self or non-self MHC-restricted peptides [58].

The implication of adaptive-like $\gamma\delta$ T lymphocytes in the antiviral response is supported by the rise of the $\gamma\delta$ TEM/TCM ratio along the course of MCMV infection. Likewise, HCMV infection induces the differentiation of non-V γ 9V δ 2 T cells from a naïve to TEMRA phenotype [29, 59]. However, in contrast to the studies in humans which describe HCMV as a major driver of TRD repertoire focusing over time in transplant patients [22, 35, 60] the overall TRD diversity in blood from long-term infected mice (d80) was similar to that of control mice. This suggests that the TRD repertoire somehow stabilizes at distance from MCMV challenge, likely due to the loss of some adaptive-like $\gamma\delta$ T cell effectors, and to the high frequency of innate like $\gamma\delta$ TEM in mice regardless of infection. Alternatively, the transplant setting in the HCMV studies may contribute to the high expansion of particular $\gamma\delta$ clonotypes. Importantly, TCR $\gamma\delta$ signaling was

essential to afford viral load control after reinfection. Whether $\gamma\delta$ T cell memory response involves TCR binding of diverse MCMV-induced antigens remains to be elucidated [16]; [61]. Counterintuitively, $\gamma\delta$ clonotypes that dominated the chronic phase of infection (d80) were not necessarily expanded in the initial phase of infection (d21). Likewise, expansion of $\gamma\delta$ T cell clonotypes after first MCMV challenge was not a prerequisite for their involvement in the secondary response. In an elegant study, the group of Buchholz recently showed that, during MCMV infection, long-term immunodominance of a single-cell derived $\alpha\beta$ T cell family is not determined by its initial expansion, but is rather predicted by its early content of T central memory precursors [62]. Moreover, inflationary KLRG1+ $\alpha\beta$ CD8 T cells have a reduced half-life and are supposed to be maintained by continuous replenishment from early primed KLRG1- $\alpha\beta$ T cells, among which $\alpha\beta$ TCM expressing Tcf1 [33, 63-66]. We hypothesize that $\gamma\delta$ TCM primed by a first MCMV encounter play a crucial role in the long-term anti-CMV response, through their capacity to proliferate and to give rise to antiviral effectors that eventually localize in target tissues or recirculate. This would explain why blocking $\gamma\delta$ TCM egress from lymph nodes does not affect viral loads control, at least in the short term. In accordance with our hypothesis, we showed the high proliferative potential of $\gamma\delta$ TCM *in vitro*, as well as their protective function and their ability to generate KLRG1+ $\gamma\delta$ TEM upon adoptive transfer into T cell deficient hosts. Applying a second intraperitoneal injection of MCMV to primarily infected mice probably leads to the mobilization of novel $\gamma\delta$ T cell responders, thus explaining the appearance of novel $\gamma\delta$ TCR clonotypes, and to an enhanced $\gamma\delta$ T cell secondary response.

To conclude, our results uncover memory properties of TCM $\gamma\delta$ T cells in the context of a chronic viral infection. These data reveal the interest of investigating and targeting this subset of unconventional T cells in strategies aiming at improving antiviral vaccination approaches. TCM $\gamma\delta$ T cells could compensate for the defect of $\alpha\beta$ T cells in immunosuppressed individuals

and are thus of particular relevance in the context of organ or hematopoietic stem cell transplantation.

MATERIALS AND METHODS

Mice

Specific Pathogen-free, 8-12 weeks old, C57BL/6 CD3 $\epsilon^{-/-}$ [67] as well as TCR $\alpha^{-/-}$ [68] were purchased from the CDTA (Centre de Distribution, Typage et Archivage Animal, Orléans, France). Experiments were performed in an appropriate biosafety level 2 facility in compliance with governmental and institutional guidelines (Animalerie spécialisée A2, Université Bordeaux Segalen, France, approval n° B33-063-916). This study was carried out in accordance with the Ethics Review Committee of Bordeaux (2016092917471799).

Virus

MCMV (Smith strain, ATCC VR-194) was obtained from the American Type Culture Collection and propagated into BALBc mice (BALBcBy/J, Charles Rivers laboratory, Larcresle, France) as previously described. Three weeks after MCMV infection, salivary glands were collected from infected mice and used as an MCMV stock solution. Determination of virus titers was defined by standard plaque forming assay on monolayers of mouse embryonic fibroblasts (MEF). Infections were performed by intraperitoneal (i.p.) administration of desired quantity of PFU from the salivary gland viral stock.

Flow cytometry

For lung preparation, collagenase I (50 µg/ml ; Sigma) and DNase I (50 µg/ml ; Sigma) were used for 1h at 37°C. Single-cell suspension from spleen, liver and enzyme treated lung were prepared by meshing organs through 70 µm nylon cell strainers in RPMI-1640 with 8% FBS (HyClone Laboratories, GE Healthcare, Logan, Utah). After red blood cells lysis with NH₄Cl (liver) or ACK (lung), lymphocytes were isolated by a discontinuous 40/80% Percoll gradient (GE Healthcare).

For Flow cytometry analysis, before antibody staining, Fc-receptors were blocked with CD16/CD32 FcR antibody (clone 93, eBioscience™). Live/dead discrimination was performed using Fixable Viability Stain 700 (BD Horizon™) according to manufacturer's instructions.

The following monoclonal antibodies were used:

<i>Antibody</i>	<i>Fluorochrome</i>	<i>Clone</i>	<i>Concentration</i>	<i>Supplier</i>
<i>γδ</i>	BV421	GL3	0,2 mg/ml	BD Biosciences
<i>CD19</i>	BV421	6D5	0,2 mg/ml	Biolegend
<i>CD3e</i>	BV786	145-2C11	0,2 mg/ml	BD Biosciences
<i>CD44</i>	BV500	IM7	0,2 mg/ml	BD Biosciences
<i>CD62L</i>	PerCP-Cy5.5	MEL-14	0,2 mg/ml	BD Biosciences
<i>Cx3CR1</i>	PE-Cy7	SA011F11	0,2 mg/ml	Biolegend
<i>Cx3CR1</i>	PE	SA011F11	0,2 mg/ml	Biolegend
<i>Granzyme A</i>	PE	3G8.5	0,2 mg/ml	Biolegend
<i>PDI</i>	FITC	29F.1A12	0,5 mg/ml	Biolegend
<i>KLRG1</i>	APC	2F1	0,2 mg/ml	BD Biosciences
<i>KLRG1</i>	FITC	2F1	0,5 mg/ml	eBioscience

For detection of intracellular cytokines, we employed the BD Cytofix/Cytoperm™ fixation/Permeabilization kit. Cells were acquired using a LSRT Fortessa (BD Biosciences), and analyzed using FlowJo software (Tree Star).

DNA extraction and quantification of MCMV DNA copy number

Genomic DNA from organs was isolated using a Nucleospin tissue purification kit (Macherey Nagel). MCMV-DNA was quantified by real-time PCR using BIO-RAD CFX with GoTaq qPCR Master Mix (Promega) and primers specific for MCMV glycoprotein B (gB) (forward primer: GGTAAGGCGTGGACTAGCGAT and reverse primer: CTAGCTGTTTTAACGCGCGG). Samples were distributed by Eppendorf epMotion 5073 automated pipetting. PCR condition was as follows: 95°C for 10 min, denaturation at 95°C for 15 s, and annealing/extension at 60°C for 1 min. Known quantities of plasmid comprising MCMV gB were used for the titration curve.

Adoptive transfer of sorted $\gamma\delta$ T cells

$\gamma\delta$ T cells were sorted from the spleen of MCMV infected or control TCR $\alpha^{-/-}$ mice using the TCR $\gamma\delta$ T cell Isolation kit (Miltenyi Biotec). For $\gamma\delta$ TCM and TEM sorting, purified $\gamma\delta$ T cells were stained and isolated using FACS Aria II Sorter (BD Biosciences). Purity was > 95%. Recipient CD3 $\epsilon^{-/-}$ mice received intravenous (i.v.) injections of a defined number of total $\gamma\delta$ T cells or of memory $\gamma\delta$ T cell populations. These animals were infected with 2.10³ pfu of MCMV the day after and followed twice a week. Mice were sacrificed when losing 10 % of their original weight or when showing signs of distress.

In vivo treatment with anti- $\gamma\delta$ TCR mAb

At day 92 post MCMV infection, TCR $\alpha^{-/-}$ mice received 200 μ g/mouse of purified Hamster anti-mouse $\gamma\delta$ T-Cell Receptor (Clone GL3) mAb, or Hamster IgG2, κ Isotype Control (Clone B81). Treatment efficiency was tested by FACS analysis in blood and organs.

AST and ALT quantifications

Mice were bled via the retro-orbital sinus after anesthesia. Serums were collected and frozen before quantification using a clinical chemistry analyzer (Horiba Pentra C400).

Anti-CD45 Intravascular staining

For in vivo antibody labelling, a total of 10 µg/100 µl of anti-CD45 APC (clone 30-F11 from eBioscience ; 0,2 mg/ml) was injected i.v to anesthetized mice via the retro-orbital venous plexus as previously described [69]. Antibody was allowed to circulate for 5 min to label cell in circulation or closely related to the vascular space. After this lapse-time, animals were sacrificed. Spleen, liver and lung were removed. Cells were isolated for ex vivo labelling before flow cytometry.

FTY720 Treatment

To prevent lymphocyte recirculation and egress from lymph nodes, the S1P1R agonist, FTY720 (2- amino-2-[2-(4-octylphenyl)ethyl]-1,3-propanediol) was used. FTY720 (Sigma-Aldrich) was reconstituted in ethanol and diluted in 2% β-cyclodextrin (Sigma-Aldrich) for injections. Long-term MCMV infected TCRα^{-/-} mice (d92 post primary infection) received every other day i.p. injections of FTY720 at a dose of 1 mg/kg, or of vehicle control containing 2.5% ethanol and 2% β-cyclodextrin. FTY720 was administered for a period of 11 days. Cells from spleen, liver and lung were analyzed one day after the final FTY720 injection.

Multiplex gene expression analysis

γδ T cells were sorted from the lung and liver of TCRα^{-/-} mice (n=10), using the TCR γδ T cell Isolation kit (Miltenyi Biotec). RNA was extracted using the Nucleospin RNAII kit (Macherey Nagel), was quantified with a NanoDrop spectrophotometer (Promega), and was qualified with the 2100 Bioanalyzer System (Agilent). The nCounter GX analysis system (NanoString) was

utilized according to the manufacturer's directions to quantify RNA expression of 547 genes on the nCounter® Immunology Panel.

CDR3 TCR δ (TRD) high-throughput sequencing

RNA was prepared from blood (250 μ l) of individual mice using QIAmp RNA Blood kit (Qiagen) and NucleoSpin RNA blood kit (Macherey Nagel), or from sorted $\gamma\delta$ T cells as above. cDNA was generated performing a template switch anchored RT-PCR. RNA was reverse transcribed via a template-switch cDNA reaction using 5' CDS oligo (dT), a template-switch adaptor (5'-AAGCAGTGGTATCAACGCAGAGTACATrGrGrG) and the Superscript II RT enzyme (Invitrogen). The cDNA was then purified using AMPure XP Beads (Agencourt). Amplification of the TRD region was achieved using a specific TRDC primer (5'-*GTCTCGTGGGCTCGGAGATGTGTATAAGAGACAGAAAACAGATGGTTTGGCCGGA*, adapter in italic) and a primer complementary to the template-switch adaptor (5'-*TCGTCGGCAGCGTCAGATGTGTATAAGAGACAGAAGCAGTGGTATCAACGCAG*, adapter in italic) with the KAPA Real-Time Library Amplification Kit (Kapa Biosystems). Adapters were required for subsequent sequencing reactions. After purification with AMPure XP beads, an index PCR with Illumina sequencing adapters was performed using the Nextera XT Index Kit. This second PCR product was again purified with AMPure XP beads. High-throughput sequencing of the generated amplicon products containing the TRG and TRD sequences was performed on an Illumina MiSeq platform using the V2 300 kit, with 150 base pairs (bp) at the 3' end (read 2) and 150 bp at the 5' end (read 1) [at the GIGA center, University of Liège, Belgium].

Raw sequencing reads from fastq files (read 1 and read 2) were aligned to reference V, D and J genes from GenBank database specifically for 'TRD' to build CDR3 sequences using the MiXCR software version 3.0.13 [70]. Default parameters were used except to assemble TRDD

gene segment where 3 instead of 5 consecutive nucleotides were applied as assemble parameter. CDR3 sequences were then exported and analyzed using VDJtools software version 1.2.1 using default settings [71]. Sequences out of frame and containing stop codons were excluded from the analysis. Note that the nucleotide lengths generated by VDJtools include the C and V ends of the CDR3 clonotypes. The degree of TCR repertoire overlap between two different samples was analyzed using the overlap F metrics calculated with the software package VDJtools (<https://vdjtools-doc.readthedocs.io/en/master/index.html>).

Statistical analysis

Statistical studies were performed using GraphPad Prism 6 software and indicated in the Figure legends (*P <0,05; **P <0.01 ***P <0.001 and ****P <0.0001).

ACKNOWLEDGMENTS

We thank Isabelle Douchet at Immunoconcept for technical assistance during mice dissection.

REFERENCES

1. Farber DL, Netea MG, Radbruch A, Rajewsky K, Zinkernagel RM. Immunological memory: lessons from the past and a look to the future. *Nat Rev Immunol*. 2016;16(2):124-8. doi: 10.1038/nri.2016.13. PubMed PMID: 26831526.
2. Pradeu T, Du Pasquier L. Immunological memory: What's in a name? *Immunol Rev*. 2018;283(1):7-20. doi: 10.1111/imr.12652. PubMed PMID: 29664563.
3. Netea MG, Schlitzer A, Placek K, Joosten LAB, Schultze JL. Innate and Adaptive Immune Memory: an Evolutionary Continuum in the Host's Response to Pathogens. *Cell Host Microbe*. 2019;25(1):13-26. doi: 10.1016/j.chom.2018.12.006. PubMed PMID: 30629914.
4. Martin MD, Badovinac VP. Defining Memory CD8 T Cell. *Front Immunol*. 2018;9:2692. doi: 10.3389/fimmu.2018.02692. PubMed PMID: 30515169; PubMed Central PMCID: PMC6255921.

5. Jameson SC, Masopust D. Understanding Subset Diversity in T Cell Memory. *Immunity*. 2018;48(2):214-26. doi: 10.1016/j.immuni.2018.02.010. PubMed PMID: 29466754; PubMed Central PMCID: PMC5863745.
6. Takamura S. Divergence of Tissue-Memory T Cells: Distribution and Function-Based Classification. *Cold Spring Harb Perspect Biol*. 2020;12(10). doi: 10.1101/cshperspect.a037762. PubMed PMID: 32816841; PubMed Central PMCID: PMC7528850.
7. Chung HK, McDonald B, Kaech SM. The architectural design of CD8+ T cell responses in acute and chronic infection: Parallel structures with divergent fates. *J Exp Med*. 2021;218(4). doi: 10.1084/jem.20201730. PubMed PMID: 33755719; PubMed Central PMCID: PMC7992501
8. Klenerman P. The (gradual) rise of memory inflation. *Immunol Rev*. 2018;283(1):99-112. doi: 10.1111/imr.12653. PubMed PMID: 29664577; PubMed Central PMCID: PMC5947157.
9. Welten SPM, Baumann NS, Oxenius A. Fuel and brake of memory T cell inflation. *Med Microbiol Immunol*. 2019;208(3-4):329-38. doi: 10.1007/s00430-019-00587-9. PubMed PMID: 30852648.
10. van den Berg SPH, Pardieck IN, Lanfermeijer J, Sauce D, Klenerman P, van Baarle D, et al. The hallmarks of CMV-specific CD8 T-cell differentiation. *Med Microbiol Immunol*. 2019;208(3-4):365-73. doi: 10.1007/s00430-019-00608-7. PubMed PMID: 30989333; PubMed Central PMCID: PMC6647465.
11. Jackson SE, Sedikides GX, Okecha G, Wills MR. Generation, maintenance and tissue distribution of T cell responses to human cytomegalovirus in lytic and latent infection. *Med Microbiol Immunol*. 2019;208(3-4):375-89. doi: 10.1007/s00430-019-00598-6. PubMed PMID: 30895366; PubMed Central PMCID: PMC6647459.
12. Hayday AC. Gammadelta T cells and the lymphoid stress-surveillance response. *Immunity*. 2009;31(2):184-96. doi: 10.1016/j.immuni.2009.08.006. PubMed PMID: 19699170.
13. Lalor SJ, McLoughlin RM. Memory gammadelta T Cells-Newly Appreciated Protagonists in Infection and Immunity. *Trends Immunol*. 2016;37(10):690-702. doi: 10.1016/j.it.2016.07.006. PubMed PMID: 27567182.
14. Khairallah C, Chu TH, Sheridan BS. Tissue Adaptations of Memory and Tissue-Resident Gamma Delta T Cells. *Front Immunol*. 2018;9:2636. doi: 10.3389/fimmu.2018.02636. PubMed PMID: 30538697; PubMed Central PMCID: PMC6277633.
15. Comeau K, Paradis P, Schiffrin EL. Human and murine memory gammadelta T cells: Evidence for acquired immune memory in bacterial and viral infections and autoimmunity. *Cell Immunol*. 2020;357:104217. doi: 10.1016/j.cellimm.2020.104217. PubMed PMID: 32979762.
16. Hayday AC. gammadelta T Cell Update: Adaptate Orchestrators of Immune Surveillance. *J Immunol*. 2019;203(2):311-20. doi: 10.4049/jimmunol.1800934. PubMed PMID: 31285310.
17. Papadopoulou M, Sanchez Sanchez G, Vermijlen D. Innate and adaptive gammadelta T cells: How, when, and why. *Immunol Rev*. 2020;298(1):99-116. doi: 10.1111/imr.12926. PubMed PMID: 33146423.
18. Willcox CR, Mohammed F, Willcox BE. The distinct MHC-unrestricted immunobiology of innate-like and adaptive-like human gammadelta T cell subsets-Nature's CAR-T cells. *Immunol Rev*. 2020;298(1):25-46. doi: 10.1111/imr.12928. PubMed PMID: 33084045.
19. Prinz I, Silva-Santos B, Pennington DJ. Functional development of gammadelta T cells. *Eur J Immunol*. 2013;43(8):1988-94. doi: 10.1002/eji.201343759. PubMed PMID: 23928962.
20. Vermijlen D, Prinz I. Ontogeny of Innate T Lymphocytes - Some Innate Lymphocytes are More Innate than Others. *Front Immunol*. 2014;5:486. doi: 10.3389/fimmu.2014.00486. PubMed PMID: 25346734; PubMed Central PMCID: PMC4193329.
21. Parker ME, Ciofani M. Regulation of gammadelta T Cell Effector Diversification in the Thymus. *Front Immunol*. 2020;11:42. doi: 10.3389/fimmu.2020.00042. PubMed PMID: 32038664; PubMed Central PMCID: PMC6992645.
22. Ravens S, Schultze-Florey C, Raha S, Sandrock I, Drenker M, Oberdorfer L, et al. Human gammadelta T cells are quickly reconstituted after stem-cell transplantation and show adaptive clonal

- expansion in response to viral infection. *Nat Immunol.* 2017;18(4):393-401. doi: 10.1038/ni.3686. PubMed PMID: 28218745.
23. Khairallah C, Dechanet-Merville J, Capone M. gammadelta T Cell-Mediated Immunity to Cytomegalovirus Infection. *Front Immunol.* 2017;8:105. doi: 10.3389/fimmu.2017.00105. PubMed PMID: 28232834; PubMed Central PMCID: PMC5298998.
24. Kaminski H, Marseres G, Cosentino A, Guerville F, Pitard V, Fournie JJ, et al. Understanding human gammadelta T cell biology toward a better management of cytomegalovirus infection. *Immunol Rev.* 2020;298(1):264-88. doi: 10.1111/imr.12922. PubMed PMID: 33091199.
25. Lafarge X, Merville P, Cazin MC, Berge F, Potaux L, Moreau JF, et al. Cytomegalovirus infection in transplant recipients resolves when circulating gammadelta T lymphocytes expand, suggesting a protective antiviral role. *J Infect Dis.* 2001;184(5):533-41. doi: 10.1086/322843. PubMed PMID: 11494158.
26. Kaminski H, Garrigue I, Couzi L, Taton B, Bachelet T, Moreau JF, et al. Surveillance of gammadelta T Cells Predicts Cytomegalovirus Infection Resolution in Kidney Transplants. *J Am Soc Nephrol.* 2016;27(2):637-45. doi: 10.1681/ASN.2014100985. PubMed PMID: 26054538; PubMed Central PMCID: PMC4731109.
27. Khairallah C, Netzer S, Villacreses A, Juzan M, Rousseau B, Dulanto S, et al. gammadelta T cells confer protection against murine cytomegalovirus (MCMV). *PLoS Pathog.* 2015;11(3):e1004702. doi: 10.1371/journal.ppat.1004702. PubMed PMID: 25747674; PubMed Central PMCID: PMC4352080.
28. Sell S, Dietz M, Schneider A, Holtappels R, Mach M, Winkler TH. Control of murine cytomegalovirus infection by gammadelta T cells. *PLoS Pathog.* 2015;11(2):e1004481. doi: 10.1371/journal.ppat.1004481. PubMed PMID: 25658831; PubMed Central PMCID: PMC4450058.
29. Pitard V, Roumanes D, Lafarge X, Couzi L, Garrigue I, Lafon ME, et al. Long-term expansion of effector/memory Vdelta2-gammadelta T cells is a specific blood signature of CMV infection. *Blood.* 2008;112(4):1317-24. doi: 10.1182/blood-2008-01-136713. PubMed PMID: 18539896; PubMed Central PMCID: PMC2515135.
30. Guo Z, Zhang Z, Prajapati M, Li Y. Lymphopenia Caused by Virus Infections and the Mechanisms Beyond. *Viruses.* 2021;13(9). doi: 10.3390/v13091876. PubMed PMID: 34578457; PubMed Central PMCID: PMC8473169.
31. Lombes A, Durand A, Charvet C, Riviere M, Bonilla N, Auffray C, et al. Adaptive Immune-like gamma/delta T Lymphocytes Share Many Common Features with Their alpha/beta T Cell Counterparts. *J Immunol.* 2015;195(4):1449-58. doi: 10.4049/jimmunol.1500375. PubMed PMID: 26123353.
32. Ibegbu CC, Xu YX, Harris W, Maggio D, Miller JD, Kourtis AP. Expression of killer cell lectin-like receptor G1 on antigen-specific human CD8+ T lymphocytes during active, latent, and resolved infection and its relation with CD57. *J Immunol.* 2005;174(10):6088-94. doi: 10.4049/jimmunol.174.10.6088. PubMed PMID: 15879103.
33. Snyder CM, Cho KS, Bonnett EL, van Dommelen S, Shellam GR, Hill AB. Memory inflation during chronic viral infection is maintained by continuous production of short-lived, functional T cells. *Immunity.* 2008;29(4):650-9. doi: 10.1016/j.immuni.2008.07.017. PubMed PMID: 18957267; PubMed Central PMCID: PMC2583440.
34. Vermijlen D, Brouwer M, Donner C, Liesnard C, Tackoen M, Van Rysselberge M, et al. Human cytomegalovirus elicits fetal gammadelta T cell responses in utero. *J Exp Med.* 2010;207(4):807-21. doi: 10.1084/jem.20090348. PubMed PMID: 20368575; PubMed Central PMCID: PMC2856038.
35. Davey MS, Willcox CR, Joyce SP, Ladell K, Kasatskaya SA, McLaren JE, et al. Clonal selection in the human Vdelta1 T cell repertoire indicates gammadelta TCR-dependent adaptive immune surveillance. *Nat Commun.* 2017;8:14760. doi: 10.1038/ncomms14760. PubMed PMID: 28248310; PubMed Central PMCID: PMC5337994.
36. Gerlach C, Moseman EA, Loughhead SM, Alvarez D, Zwijnenburg AJ, Waanders L, et al. The Chemokine Receptor CX3CR1 Defines Three Antigen-Experienced CD8 T Cell Subsets with Distinct Roles in Immune Surveillance and Homeostasis. *Immunity.* 2016;45(6):1270-84. doi: 10.1016/j.immuni.2016.10.018. PubMed PMID: 27939671; PubMed Central PMCID: PMC5177508.

37. Koenecke C, Chennupati V, Schmitz S, Malissen B, Forster R, Prinz I. In vivo application of mAb directed against the gammadelta TCR does not deplete but generates "invisible" gammadelta T cells. *Eur J Immunol.* 2009;39(2):372-9. doi: 10.1002/eji.200838741. PubMed PMID: 19130484.
38. Chen HC, Eling N, Martinez-Jimenez CP, O'Brien LM, Carbonaro V, Marioni JC, et al. IL-7-dependent compositional changes within the gammadelta T cell pool in lymph nodes during ageing lead to an unbalanced anti-tumour response. *EMBO Rep.* 2019;20(8):e47379. doi: 10.15252/embr.201847379. PubMed PMID: 31283095; PubMed Central PMCID: PMC6680116.
39. Paget C, Chow MT, Gherardin NA, Beavis PA, Uldrich AP, Duret H, et al. CD3bright signals on gammadelta T cells identify IL-17A-producing Vgamma6Vdelta1+ T cells. *Immunol Cell Biol.* 2015;93(2):198-212. doi: 10.1038/icb.2014.94. PubMed PMID: 25385067.
40. Dillen CA, Pinsker BL, Marusina AI, Merleev AA, Farber ON, Liu H, et al. Clonally expanded gammadelta T cells protect against *Staphylococcus aureus* skin reinfection. *J Clin Invest.* 2018;128(3):1026-42. doi: 10.1172/JCI96481. PubMed PMID: 29400698; PubMed Central PMCID: PMC5824877.
41. Marchitto MC, Dillen CA, Liu H, Miller RJ, Archer NK, Ortines RV, et al. Clonal Vgamma6(+)Vdelta4(+) T cells promote IL-17-mediated immunity against *Staphylococcus aureus* skin infection. *Proc Natl Acad Sci U S A.* 2019;116(22):10917-26. doi: 10.1073/pnas.1818256116. PubMed PMID: 31088972; PubMed Central PMCID: PMC6561199.
42. Khairallah C, Bettke JA, Gorbatshevych O, Qiu Z, Zhang Y, Cho K, et al. A blend of broadly-reactive and pathogen-selected Vgamma4 Vdelta1 T cell receptors confer broad bacterial reactivity of resident memory gammadelta T cells. *Mucosal Immunol.* 2022;15(1):176-87. doi: 10.1038/s41385-021-00447-x. PubMed PMID: 34462572; PubMed Central PMCID: PMC8738109.
43. Pereira P, Berthault C, Burlen-Defranoux O, Boucontet L. Critical role of TCR specificity in the development of Vgamma1Vdelta6.3+ innate NKTgammadelta cells. *J Immunol.* 2013;191(4):1716-23. doi: 10.4049/jimmunol.1203168. PubMed PMID: 23851687.
44. Mamedov MR, Scholzen A, Nair RV, Cumnock K, Kenkel JA, Oliveira JHM, et al. A Macrophage Colony-Stimulating-Factor-Producing gammadelta T Cell Subset Prevents Malarial Parasitemic Recurrence. *Immunity.* 2018;48(2):350-63 e7. doi: 10.1016/j.immuni.2018.01.009. PubMed PMID: 29426701; PubMed Central PMCID: PMC5956914.
45. Lefranc MP. Immunoglobulin and T Cell Receptor Genes: IMGT((R)) and the Birth and Rise of Immunoinformatics. *Front Immunol.* 2014;5:22. doi: 10.3389/fimmu.2014.00022. PubMed PMID: 24600447; PubMed Central PMCID: PMC3913909.
46. Snyder CM, Cho KS, Bonnett EL, Allan JE, Hill AB. Sustained CD8+ T cell memory inflation after infection with a single-cycle cytomegalovirus. *PLoS Pathog.* 2011;7(10):e1002295. doi: 10.1371/journal.ppat.1002295. PubMed PMID: 21998590; PubMed Central PMCID: PMC3188546.
47. Gordon CL, Lee LN, Swadling L, Hutchings C, Zinser M, Highton AJ, et al. Induction and Maintenance of CX3CR1-Intermediate Peripheral Memory CD8(+) T Cells by Persistent Viruses and Vaccines. *Cell Rep.* 2018;23(3):768-82. doi: 10.1016/j.celrep.2018.03.074. PubMed PMID: 29669283; PubMed Central PMCID: PMC5917822.
48. Redeker A, Welten SP, Arens R. Viral inoculum dose impacts memory T-cell inflation. *Eur J Immunol.* 2014;44(4):1046-57. doi: 10.1002/eji.201343946. PubMed PMID: 24356925.
49. Holtappels R, Freitag K, Renzaho A, Becker S, Lemmermann NAW, Reddehase MJ. Revisiting CD8 T-cell 'Memory Inflation': New Insights with Implications for Cytomegaloviruses as Vaccine Vectors. *Vaccines (Basel).* 2020;8(3). doi: 10.3390/vaccines8030402. PubMed PMID: 32707744; PubMed Central PMCID: PMC7563500.
50. Welten SPM, Oderbolz J, Yilmaz V, Bidgood SR, Gould V, Mercer J, et al. Influenza- and MCMV-induced memory CD8 T cells control respiratory vaccinia virus infection despite residence in distinct anatomical niches. *Mucosal Immunol.* 2021;14(3):728-42. doi: 10.1038/s41385-020-00373-4. PubMed PMID: 33479479; PubMed Central PMCID: PMC8075924.
51. Wirth TC, Xue HH, Rai D, Sabel JT, Bair T, Harty JT, et al. Repetitive antigen stimulation induces stepwise transcriptome diversification but preserves a core signature of memory CD8(+) T cell

differentiation. *Immunity*. 2010;33(1):128-40. doi: 10.1016/j.immuni.2010.06.014. PubMed PMID: 20619696; PubMed Central PMCID: PMC2912220.

52. Hoft DF, Brown RM, Roodman ST. Bacille Calmette-Guerin vaccination enhances human gamma delta T cell responsiveness to mycobacteria suggestive of a memory-like phenotype. *J Immunol*. 1998;161(2):1045-54. PubMed PMID: 9670986.

53. Lai X, Shen Y, Zhou D, Sehgal P, Shen L, Simon M, et al. Immune biology of macaque lymphocyte populations during mycobacterial infection. *Clin Exp Immunol*. 2003;133(2):182-92. doi: 10.1046/j.1365-2249.2003.02209.x. PubMed PMID: 12869023; PubMed Central PMCID: PMC1808757.

54. Ryan-Payseur B, Frencher J, Shen L, Chen CY, Huang D, Chen ZW. Multieffector-functional immune responses of HMBPP-specific Vgamma2Vdelta2 T cells in nonhuman primates inoculated with *Listeria monocytogenes* DeltaactA prfA*. *J Immunol*. 2012;189(3):1285-93. doi: 10.4049/jimmunol.1200641. PubMed PMID: 22745375; PubMed Central PMCID: PMC3412419.

55. Sheridan BS, Romagnoli PA, Pham QM, Fu HH, Alonzo F, 3rd, Schubert WD, et al. gammadelta T cells exhibit multifunctional and protective memory in intestinal tissues. *Immunity*. 2013;39(1):184-95. doi: 10.1016/j.immuni.2013.06.015. PubMed PMID: 23890071; PubMed Central PMCID: PMC3749916.

56. Romagnoli PA, Sheridan BS, Pham QM, Lefrancois L, Khanna KM. IL-17A-producing resident memory gammadelta T cells orchestrate the innate immune response to secondary oral *Listeria monocytogenes* infection. *Proc Natl Acad Sci U S A*. 2016;113(30):8502-7. doi: 10.1073/pnas.1600713113. PubMed PMID: 27402748; PubMed Central PMCID: PMC4968747.

57. Tieppo P, Papadopoulou M, Gatti D, McGovern N, Chan JKY, Gosselin F, et al. The human fetal thymus generates invariant effector gammadelta T cells. *J Exp Med*. 2020;217(3). doi: 10.1084/jem.20190580. PubMed PMID: 31816633; PubMed Central PMCID: PMC7062527.

58. Madi A, Poran A, Shifrut E, Reich-Zeliger S, Greenstein E, Zaretsky I, et al. T cell receptor repertoires of mice and humans are clustered in similarity networks around conserved public CDR3 sequences. *Elife*. 2017;6. doi: 10.7554/eLife.22057. PubMed PMID: 28731407; PubMed Central PMCID: PMC5553937.

59. Couzi L, Pitard V, Netzer S, Garrigue I, Lafon ME, Moreau JF, et al. Common features of gammadelta T cells and CD8(+) alphabeta T cells responding to human cytomegalovirus infection in kidney transplant recipients. *J Infect Dis*. 2009;200(9):1415-24. doi: 10.1086/644509. PubMed PMID: 19780672.

60. Dechanet J, Merville P, Lim A, Retiere C, Pitard V, Lafarge X, et al. Implication of gammadelta T cells in the human immune response to cytomegalovirus. *J Clin Invest*. 1999;103(10):1437-49. doi: 10.1172/JCI5409. PubMed PMID: 10330426; PubMed Central PMCID: PMC408467.

61. Hayday AC, Vantourout P. The Innate Biologies of Adaptive Antigen Receptors. *Annu Rev Immunol*. 2020;38:487-510. doi: 10.1146/annurev-immunol-102819-023144. PubMed PMID: 32017636.

62. Grassmann S, Mihatsch L, Mir J, Kazeroonian A, Rahimi R, Flommersfeld S, et al. Early emergence of T central memory precursors programs clonal dominance during chronic viral infection. *Nat Immunol*. 2020;21(12):1563-73. doi: 10.1038/s41590-020-00807-y. PubMed PMID: 33106669.

63. Torti N, Walton SM, Brocker T, Rulicke T, Oxenius A. Non-hematopoietic cells in lymph nodes drive memory CD8 T cell inflation during murine cytomegalovirus infection. *PLoS Pathog*. 2011;7(10):e1002313. doi: 10.1371/journal.ppat.1002313. PubMed PMID: 22046127; PubMed Central PMCID: PMC3203160.

64. Quinn M, Turula H, Tandon M, Deslouches B, Moghbeli T, Snyder CM. Memory T cells specific for murine cytomegalovirus re-emerge after multiple challenges and recapitulate immunity in various adoptive transfer scenarios. *J Immunol*. 2015;194(4):1726-36. doi: 10.4049/jimmunol.1402757. PubMed PMID: 25595792; PubMed Central PMCID: PMC4684174.

65. Baumann NS, Torti N, Welten SPM, Barnstorf I, Borsa M, Pallmer K, et al. Tissue maintenance of CMV-specific inflationary memory T cells by IL-15. *PLoS Pathog*. 2018;14(4):e1006993. doi: 10.1371/journal.ppat.1006993. PubMed PMID: 29652930; PubMed Central PMCID: PMC5919076.

66. Welten SPM, Yermanos A, Baumann NS, Wagen F, Oetiker N, Sandu I, et al. Tcf1(+) cells are required to maintain the inflationary T cell pool upon MCMV infection. *Nat Commun.* 2020;11(1):2295. doi: 10.1038/s41467-020-16219-3. PubMed PMID: 32385253; PubMed Central PMCID: PMC7211020.
67. Tanaka Y, Ardouin L, Gillet A, Lin SY, Magnan A, Malissen B, et al. Early T-cell development in CD3-deficient mice. *Immunol Rev.* 1995;148:171-99. doi: 10.1111/j.1600-065x.1995.tb00098.x. PubMed PMID: 8825287.
68. Philpott KL, Viney JL, Kay G, Rastan S, Gardiner EM, Chae S, et al. Lymphoid development in mice congenitally lacking T cell receptor alpha beta-expressing cells. *Science.* 1992;256(5062):1448-52. doi: 10.1126/science.1604321. PubMed PMID: 1604321.
69. Anderson KG, Mayer-Barber K, Sung H, Beura L, James BR, Taylor JJ, et al. Intravascular staining for discrimination of vascular and tissue leukocytes. *Nat Protoc.* 2014;9(1):209-22. doi: 10.1038/nprot.2014.005. PubMed PMID: 24385150; PubMed Central PMCID: PMC4428344.
70. Bolotin DA, Poslavsky S, Mitrophanov I, Shugay M, Mamedov IZ, Putintseva EV, et al. MiXCR: software for comprehensive adaptive immunity profiling. *Nat Methods.* 2015;12(5):380-1. doi: 10.1038/nmeth.3364. PubMed PMID: 25924071.
71. Shugay M, Bagaev DV, Turchaninova MA, Bolotin DA, Britanova OV, Putintseva EV, et al. VDJtools: Unifying Post-analysis of T Cell Receptor Repertoires. *PLoS Comput Biol.* 2015;11(11):e1004503. doi: 10.1371/journal.pcbi.1004503. PubMed PMID: 2606115; PubMed Central PMCID: PMC4659587.

FIGURE CAPTIONS

Fig 1. $\gamma\delta$ T cell response to secondary MCMV challenge. (A) Experimental scheme: analyses in organs. TCR α ^{-/-} mice (n=25) were infected with MCMV (2.10³ PFU) at day 0, or left uninfected (n=25). 3 months later, uninfected mice were primarily infected, and infected mice were re-challenged with similar dose of MCMV. The kinetic of the $\gamma\delta$ T cell response was analyzed in the liver and lung and depicted longitudinally although mice (n=5) were sacrificed at indicated time points. (B, upper panels) Total number of $\gamma\delta$ T lymphocytes in organs. Data represent the mean \pm SEM of cell counts from 5 mice (1-way ANOVA). (B, lower panels) Viral loads/ 1 μ g of total DNA for individual mouse that were quantified in organs by qPCR. The median is shown by a line. (C) Longitudinal analysis of $\gamma\delta$ T cells in blood. TCR α ^{-/-} mice (n=10) were infected with MCMV (2.10³ PFU) at day 0, then re-challenged at day 92 with similar dose of MCMV. Mice were bled at the indicated time points. Mean absolute numbers \pm SEM of $\gamma\delta$ T lymphocytes in 25 μ l of blood are shown. Friedman statistical test was used

with d3 (post-primary) and d1 (post-secondary infection) as references. (A-C) The experiment was repeated twice with comparable results.

Fig 2. KLRG1+ $\gamma\delta$ TEM dominate the $\gamma\delta$ T cell secondary response to MCMV. (A) Kinetic evolution of naïve (CD44-CD62L+), TEM (CD44+CD62L-) and TCM (CD44+CD62L+) $\gamma\delta$ T cell subsets. (A, upper panel) analysis in organs. TCR α ^{-/-} mice (n=25) were infected with MCMV (2.10³ PFU) at day 0, or left uninfected (n=25). 3 months later, uninfected mice were primarily infected, and infected mice were re-challenged with similar dose of MCMV. The kinetic of the $\gamma\delta$ T cell response was analyzed in the liver and lung and depicted longitudinally although mice (n=5) were sacrificed at indicated time points. Data represent the mean +/- SEM of cell counts from 5 mice. (1-way ANOVA) (A, lower panels) Analysis in blood. TCR α ^{-/-} mice (n=10) were infected with MCMV (2.10³ PFU) at day 0, then re-challenged at day 92 with similar dose of MCMV. Mice were bled at the indicated time points. Mean absolute numbers +/- SEM of $\gamma\delta$ T lymphocytes in 25 μ l of blood are shown. Statistical test was Friedman (comparison between d3 and other days in primary infection, and d1 and other time points in secondary infection). (B) Kinetic evolution of KLRG1+ and KLRG1- $\gamma\delta$ TEM. (A-B) These experiments were repeated twice with comparable results.

Fig 3. MCMV leaves a long-lasting imprint on $\gamma\delta$ T cell phenotype. Long-term (d92) TCR α ^{-/-} MCMV infected mice (dark) were compared to age-matched uninfected TCR α ^{-/-} mice (grey). (A) Proportions of KLRG1+ CX3CR1+ and KLRG1-CX3CR1- cells among $\gamma\delta$ TEM (upper panels) and $\gamma\delta$ TCM (lower panels) from indicate samples in individual mice. (B) Intracellular Granzyme A expression in gated CX3CR1+KLRG1+ and CX3CR1-KLRG1- $\gamma\delta$ TEM populations from lung, liver and blood. Data are representative of 2 experiments. Statistical test was 1-way ANOVA.

Fig 4. $\gamma\delta$ T cells expressing KLRG1/CX3CR1 preferentially localize in the vasculature.

Long-term MCMV infected TCR $\alpha^{-/-}$ mice (INF) (n=5) or naïve age-matched control mice (UNI) (n=5) received anti-CD45 labeled mAb intravenously. Mice were sacrificed 5 min after antibody injection. (A) Repartition of $\gamma\delta$ T cells in the intravascular positive (IV+) or intravascular negative (IV-) fraction in indicated organs from infected mice. Pie charts show the mean percentages of $\gamma\delta$ T cells from 5 mice in each fraction. Representative contour plots obtained for one mouse out of 5 are shown. (B) Repartition of $\gamma\delta$ naïve, TCM and TEM in the IV+ or the IV- fraction from organs of one representative infected mouse. (C) Repartition of $\gamma\delta$ TEM subtypes within the IV+ or IV- compartment according to KLRG1 and CX3CR1 expression. (D) Comparative analyses between control uninfected (triangle) or infected (circle) mice, of the repartition of the $\gamma\delta$ T cell memory subtypes within the IV+ or IV- compartment, according to the expression of KLRG1, CX3CR1 and PD1. Data represent the mean \pm SD of proportions of $\gamma\delta$ T cell memory subsets from 5 infected mice or 5 naïve mice in one representative experiment out of 2. Statistical test was 1-way ANOVA.

Fig 5. Blocking $\gamma\delta$ TCM egress from peripheral organs poorly affects viral load control in

long-term infected mice. Long-term MCMV infected TCR $\alpha^{-/-}$ mice (n=10) were treated (n=5) or not (n=5) with FTY720 for 11 days before sacrifice. (A) Histograms show the number of $\gamma\delta$ TCM (upper panels) and TEM (lower panels) in organs (total numbers) or blood (per 25 μ l). (B) Viral loads in organs of treated or untreated mice were quantified by qPCR. Each point indicates one individual mouse and represents MCMV copy numbers in 1 μ g of total DNA. Data are pooled from two independent experiments (n = 5 per group). (A-B) Error bars represent the standard error of the mean of $\gamma\delta$ T cell numbers (A) and of the median of MCMV copy numbers (B). Differences were evaluated by the Mann-Whitney statistical test.

Fig 6. Viral control after reinfection engages $\gamma\delta$ -TCR signaling. TCR α ^{-/-} mice (n=10) were infected with MCMV (2.10³ PFU) at day 0. At day 92, mice received isotype control or anti- $\gamma\delta$ mAb (n=5). 24h after, mice were re-challenged with similar doses of MCMV. (A) Experimental scheme. (B) Staining of CD3 ϵ ⁺/ $\gamma\delta$ ⁺ cells in mice treated with anti- $\gamma\delta$ TCR or control mAb at day 7 post reinfection. (C) Viral loads/1 μ g of total DNA for individual mouse were quantified in organs by qPCR 7 days post-reinfection. Statistical tests were Mann Whitney. The experiment was repeated twice with comparable results.

Fig 7. Expansion of private CDR3 δ repertoire following MCMV infection. TCR α ^{-/-} mice (n=5) were infected with MCMV. Age matched uninfected TCR α ^{-/-} mice (n=3) were used as controls. Blood was drawn at different time intervals post-infection and at d7 post-reinfection. (A) Examples of clonotype tracking stackplots for 3 mice in the infected group and 2 mice in the control group. Detailed profiles for top 100 clonotypes, as well as collapsed (“Not-shown” in dark gray) and non-overlapping (light gray) clonotypes found in blood of MCMV-infected mice (Upper panels) or age-matched control mice (Lower panels). Clonotypes are colored by the peak position of their abundance profile. (B) Geometric mean of relative overlap frequencies (F metrics) within pairs of blood (left) or of organ (right) samples, each dot represents the F value (x100) of a pair of samples. Statistical tests were Mann Whitney. (C) Percentage of CGSDIGGSSWDTRQMFF (left), and CALWEPHIGGIRATDKLVF (right) sequences in TRD repertoire, in blood and organs from infected and naïve age matched control mice. Statistical test was 1-way ANOVA.

Fig 8. Long-term induced $\gamma\delta$ T cells confer protection to T cell deficient hosts upon adoptive transfer. (A) Experimental scheme. $\gamma\delta$ T cells were sorted from the spleen (purity > 95%) of 3 months infected TCR α ^{-/-} mice and 1.10⁶ cells were transferred into CD3 ϵ ^{-/-} mice. The day after, CD3 ϵ ^{-/-} hosts were infected with MCMV (2.10³ PFU). (B, left) Survival curve

of mice given long-term MCMV-primed $\gamma\delta$ T cells (grey line, n=14) and of CD3 ϵ ^{-/-} control mice (dark line, n=5). Mice were sacrificed when losing 10% weight. (B, right) Quantification of viral loads by qPCR, in organs from 5 T-cell deficient mice at sacrifice (dark squares) and 8 $\gamma\delta$ -bearing mice that had survived until d130 (grey circles). (C) 1.10⁶ $\gamma\delta$ T cells from age-matched TCR α ^{-/-} control mice were transferred into CD3 ϵ ^{-/-} mice that were MCMV-infected the day after. (C, upper left) Survival curve of mice given naïve $\gamma\delta$ (n=12), MCMV-primed $\gamma\delta$ (n=5), and of untransferred CD3 ϵ ^{-/-} mice (n=11). (C, upper right) Quantification of viral loads by qPCR, in organs from CD3 ϵ ^{-/-} control mice (n=11), naïve $\gamma\delta$ T cell bearing mice (n=11), and MCMV primed $\gamma\delta$ T cell bearing mice (n=3) (C, lower panels) Serum quantification of aspartate aminotransferase (ALT) and alanine aminotransferase AST (left) and number of $\gamma\delta$ T cells in blood (right) at day 30 post transfer, in 5 mice receiving naïve or MCMV-primed $\gamma\delta$ T cells. Statistical tests were Mann Whitney. Log-rank test were used for Kaplan-Meier survival curves. Survival curves and quantification of viral loads were from one representative experiment out of two.

Fig 9. The protective function of d92 MCMV-induced $\gamma\delta$ T cells from the spleen principally relies on the presence of $\gamma\delta$ TCM. (A, upper panel)) Survival curve of CD3 ϵ ^{-/-} mice given 200000 $\gamma\delta$ TCM KLRG1⁻ (n=7), $\gamma\delta$ TEM KLRG1⁻ (n=8) or $\gamma\delta$ TEM KLRG1⁺ (n=8). The experiment was repeated twice with comparative results. (A, lower panel) Quantification of viral loads by qPCR in organs from recipient mice at sacrifice. (B) Serum quantification of ALT and AST. Mice given $\gamma\delta$ TEM KLRG1⁻ and KLRG1⁺ cells were sacrificed when losing 10% weight, and mice given $\gamma\delta$ TCM KLRG1⁻ were sacrificed at the end of the experiment, at d150 (n=5). (C) Distribution of $\gamma\delta$ T cell memory subsets in organs from $\gamma\delta$ TCM recipient mice that had survived (mean numbers). Same statistical tests are as in Fig 8.

S1 Fig. kinetic evolution of the proportion of $\gamma\delta$ T cell memory subsets in organs. TCR α -/- mice (n=25) were infected with MCMV (2.10^3 PFU) at day 0, or left uninfected (n=25). 3 months later, uninfected mice were primarily infected, and infected mice were re-challenged with similar dose of MCMV. (A) Percentages of naïve (CD44-CD62L+), TCM (CD44+CD62L+) and TEM (CD44+CD62L-) cells among $\gamma\delta$ T lymphocytes from organs. (B) Percentages of KLRG1+ and KLRG1- cells among $\gamma\delta$ TEM. Data represent the mean percentages +/- SEM from 5 mice.

S2 Fig. Phenotypic analysis of $\gamma\delta$ TEM from d92 MCMV-infected and age-matched control mice. (A) Co-expression of CX3CR1 and KLRG1 on $\gamma\delta$ TEM from organs and blood of d92 MCMV-infected and age-matched control mice. (B) Mutually exclusive expression of KLRG1 and PD1 $\gamma\delta$ TEM from organs of d92 MCMV-infected and age-matched control mice. Numbers show percentages of each marker among $\gamma\delta$ TEM. One representative mouse is shown for each (control and long-term MCMV infected) group of mice.

S3 Fig. Multiplex gene expression analysis of immunology markers expressed by MCMV-induced $\gamma\delta$ T cells. $\gamma\delta$ T cells were sorted from lung and liver of TCR α -/- mice (n=10) at d0, d14 or d92 post MCMV infection, and day 7 post-reinfection (d7R). Analyses were performed with nSolver™ Analysis Software (NanoString). (A) Histograms represent transcripts shared by liver and lung, and whose d92/d0 ratios were >2 or < -2 (minimum counts=100). (B) Counts evolution of these transcripts at day 0, 14, 92 post-infection (d0, d14, d92), and day 7 post reinfection (d7R).

S4 Fig. CDR3 δ repertoire analysis. TCR α -/- mice (n=5) were infected with MCMV. Age matched uninfected TCR α -/- mice (n=3) were used as controls. Blood was drawn at different time intervals post infection. At day 7 post reinfection, blood and organs were analyzed. (A)

Comparison between infected (right panels) and age-matched control mice (left panels), of the CDR3 TRD repertoire of blood samples at d0, 21, 80 post-infection (d0, d21, d80) and at d7 post-reinfection (d7R), and from organs at d7R. (Upper panels) TRDV usage distribution, (Middle panels) CDR3 length in nucleotides (including the codons for C-start and F-end residues), each dot represents the weighted mean of an individual sample. (Lower panels) Number of N additions, each dot represents the weighted mean of an individual sample. (B) Percentage of unique clonotypes required to account for 50 % of the total repertoire in infected or age-matched control mice. Statistical test was 1-way ANOVA.

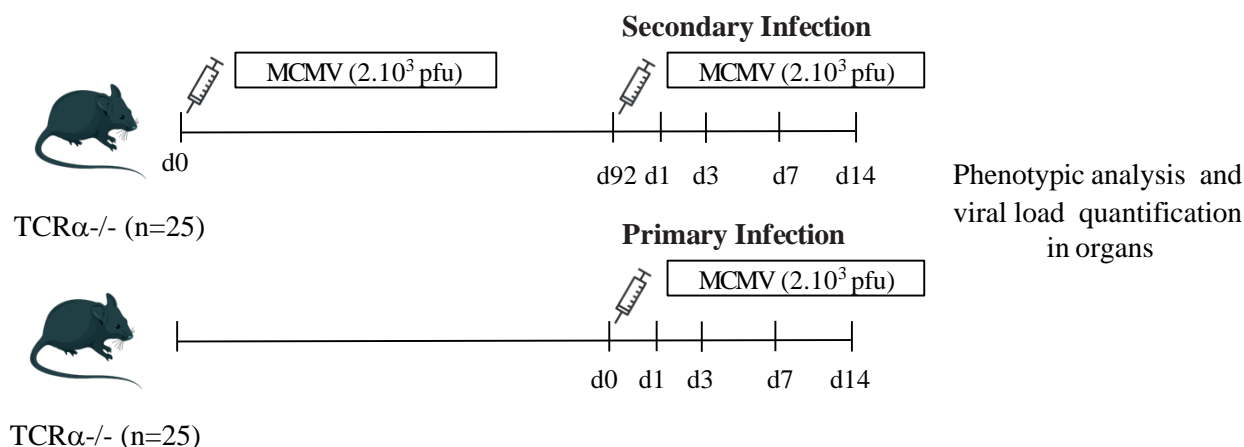
S5 Fig. Tracking of shared clonotypes after reinfection in blood and organs. TCR α ^{-/-} mice (n=5) were infected with MCMV and reinfected 3 months later. At day 7 post reinfection (d7R), blood and organs were analyzed. (Upper panels) Examples of clonotype tracking stackplots for 3 infected mice: detailed profiles for top 100 clonotypes, as well as collapsed (“NotShown” in dark gray) and non-overlapping (light gray) clonotypes found in blood and organs at d7R. Clonotypes are colored by the peak position of their abundance profile. The colors are matched for each mouse samples but not between the different mice. (Lower panels) Overlap frequencies of the D7R repertoire compared to the indicated column. Each dot corresponds to one pair comparison and one mouse. Statistical test was 1-way ANOVA.

S6 Fig. Repartition of KLRG1/CX3CR1 expressing $\gamma\delta$ T cell subtypes in $\gamma\delta$ -bearing CD3 ϵ ^{-/-} mice infected with MCMV and in d92-infected TCR α ^{-/-} mice. Long-term MCMV-induced $\gamma\delta$ T cells were sorted from the spleen of TCR α ^{-/-} mice and transferred into CD3 ϵ ^{-/-} mice that were subsequently infected with MCMV. (Upper panels) Percentages of $\gamma\delta$ TCM and TEM were determined in organs from 5 d92-infected TCR α ^{-/-} mice. (Lower panels) Percentages of $\gamma\delta$ TCM and TEM were determined in organs from 8, $\gamma\delta$ bearing CD3 ϵ ^{-/-} mice

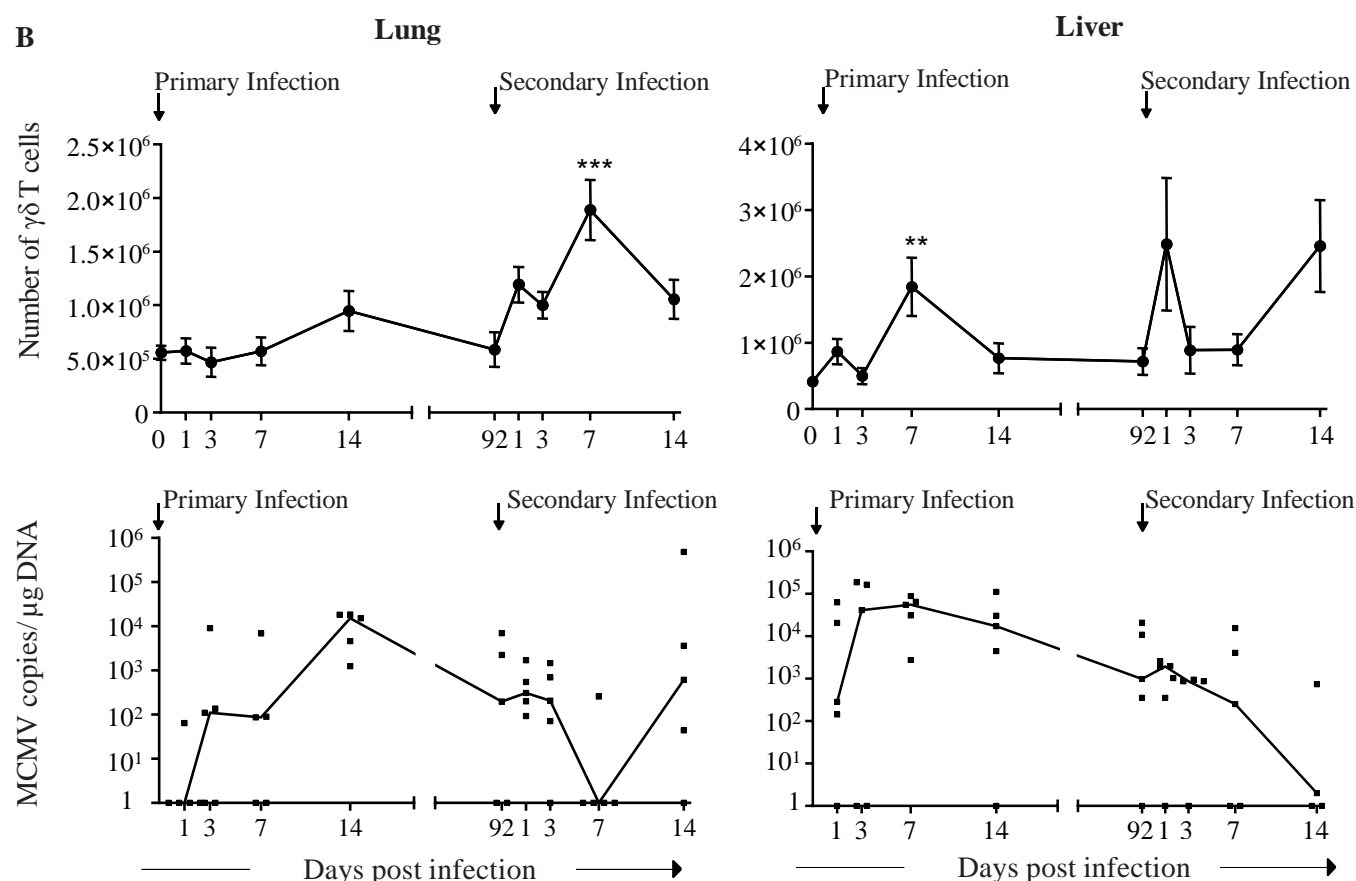
that had survived until d130. The proportion of indicated subtypes within total TCM and TEM is shown by shades of grey.

S7 Fig. $\gamma\delta$ TCM are more proliferative than $\gamma\delta$ TEM in response to IL15. Total $\gamma\delta$ T cells were sorted from the spleen of 3 months infected TCR $\alpha^{-/-}$ mice. Cells were labelled with CTY and cultured with or without IL15 (200 ng/ μ l) for 3 days. (A) Percentages of viable cells among $\gamma\delta$ T cells cultured in the absence or presence of IL15. (B) Percentages of proliferative $\gamma\delta$ TCM or TEM after 3 days of culture with IL15 (C) Representative histograms of cellular proliferation for TCM (light grey) and TEM (dark grey) from d92-infected TCR $\alpha^{-/-}$ mice. Data are representative of 3 independent experiments.

A



B



C

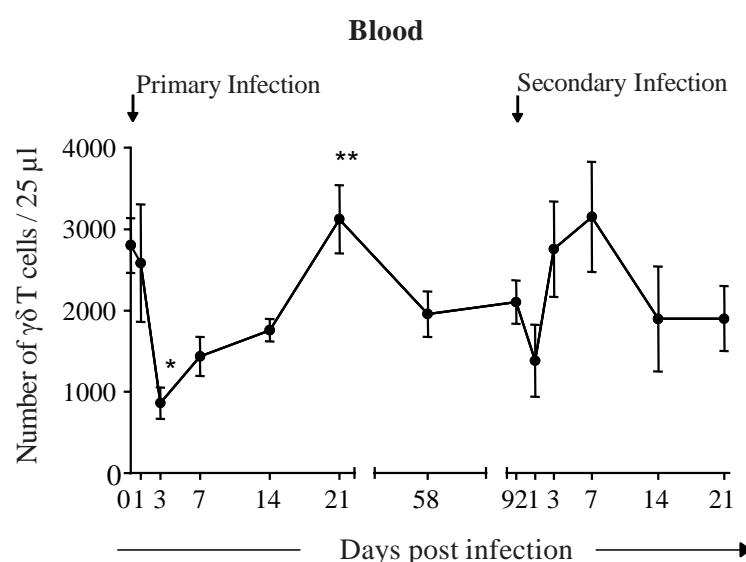


Fig 1

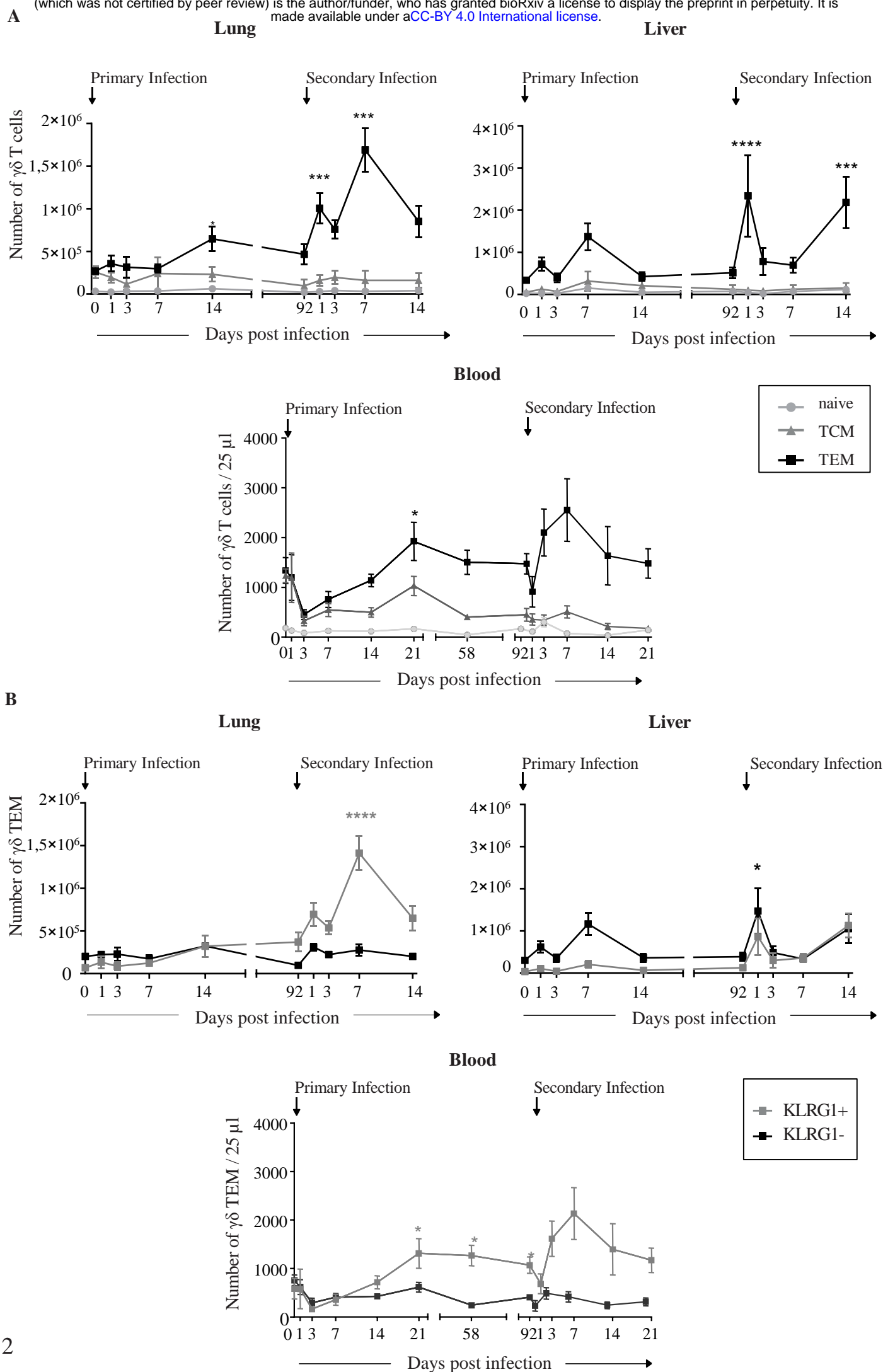


Fig 2

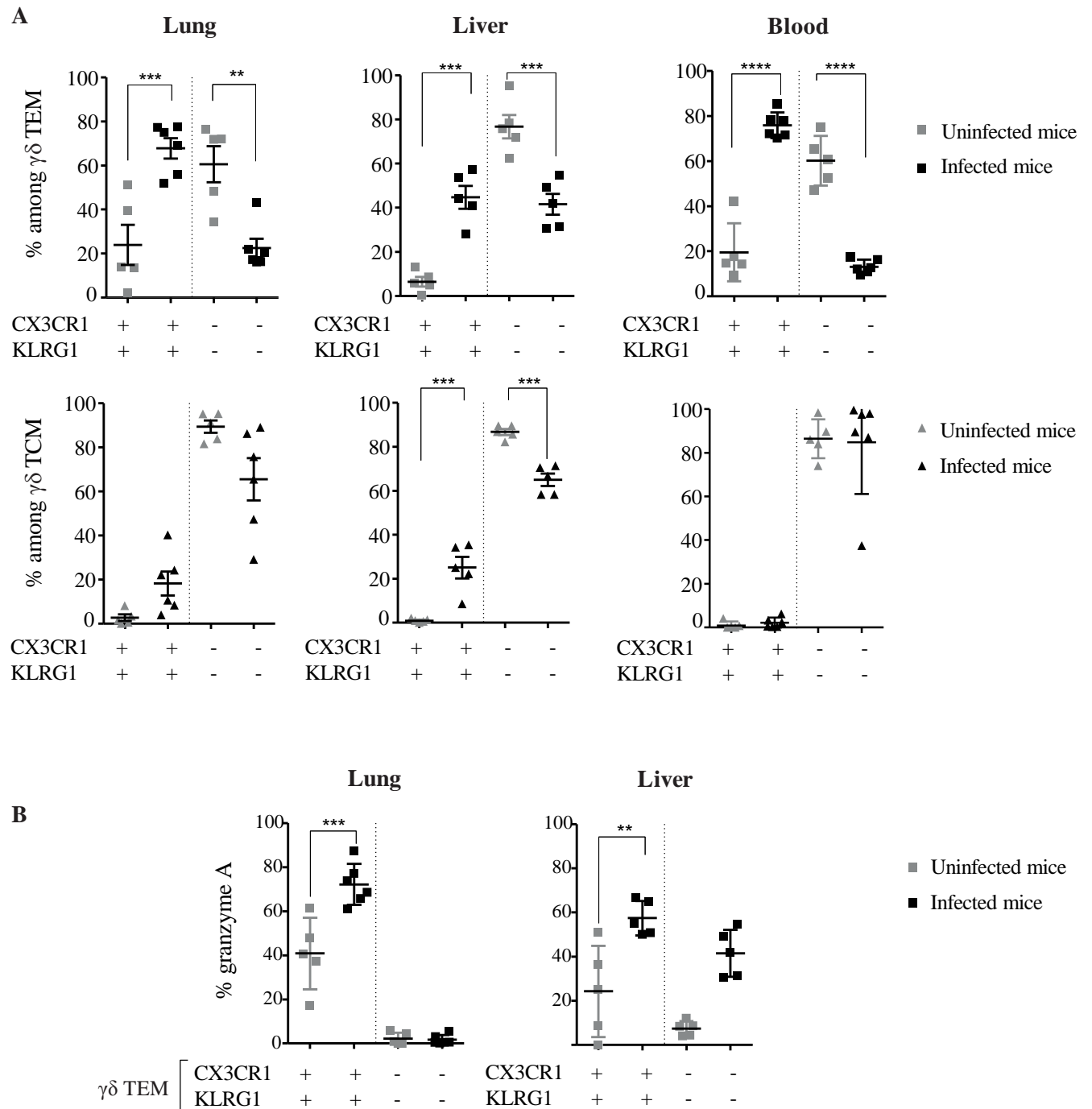


Fig 3

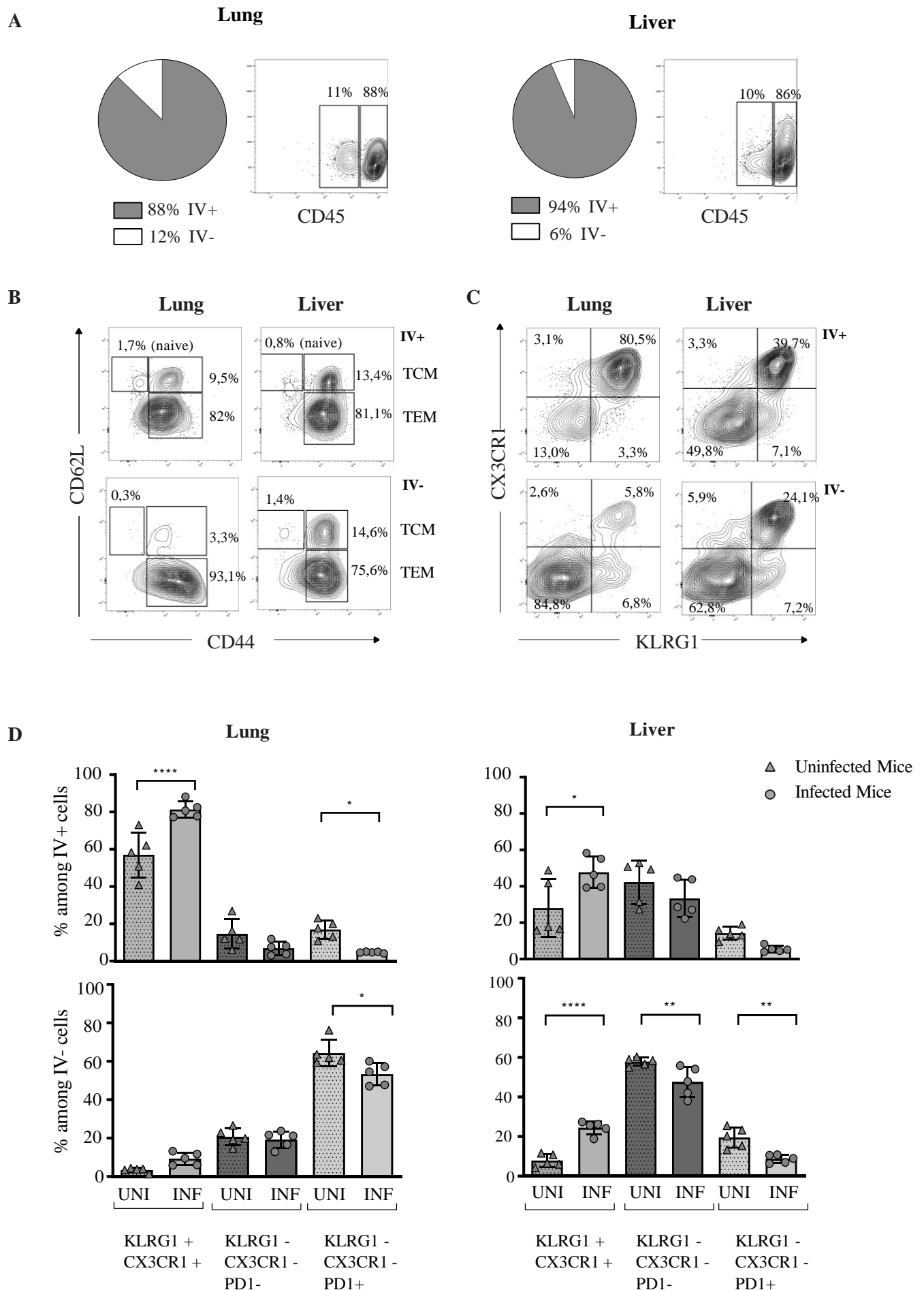


Fig 4

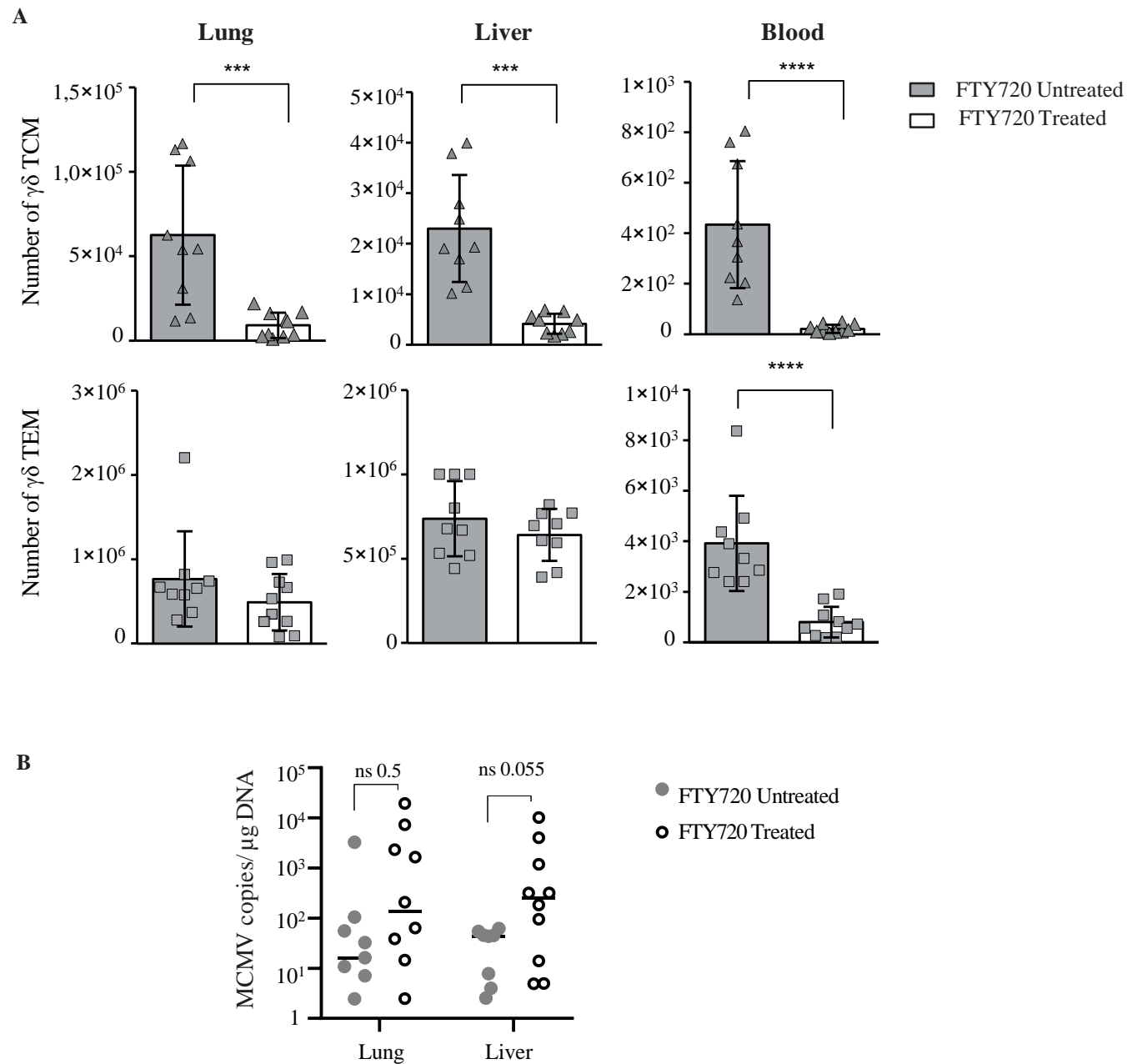
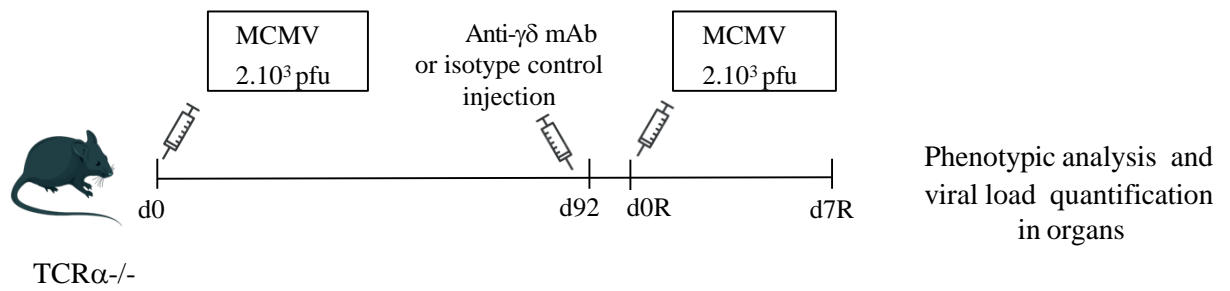
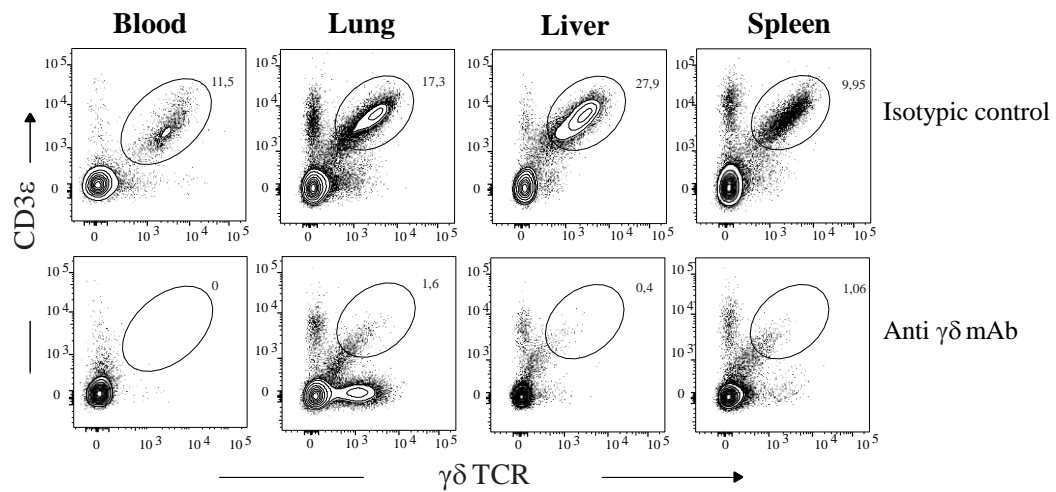


Fig 5

A



B



C

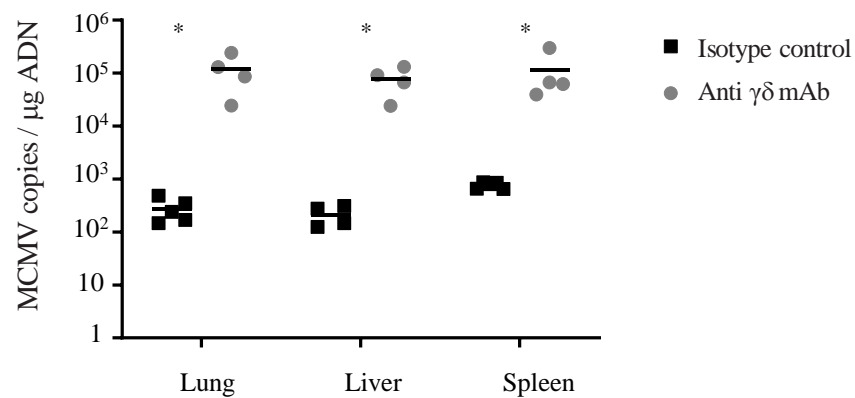
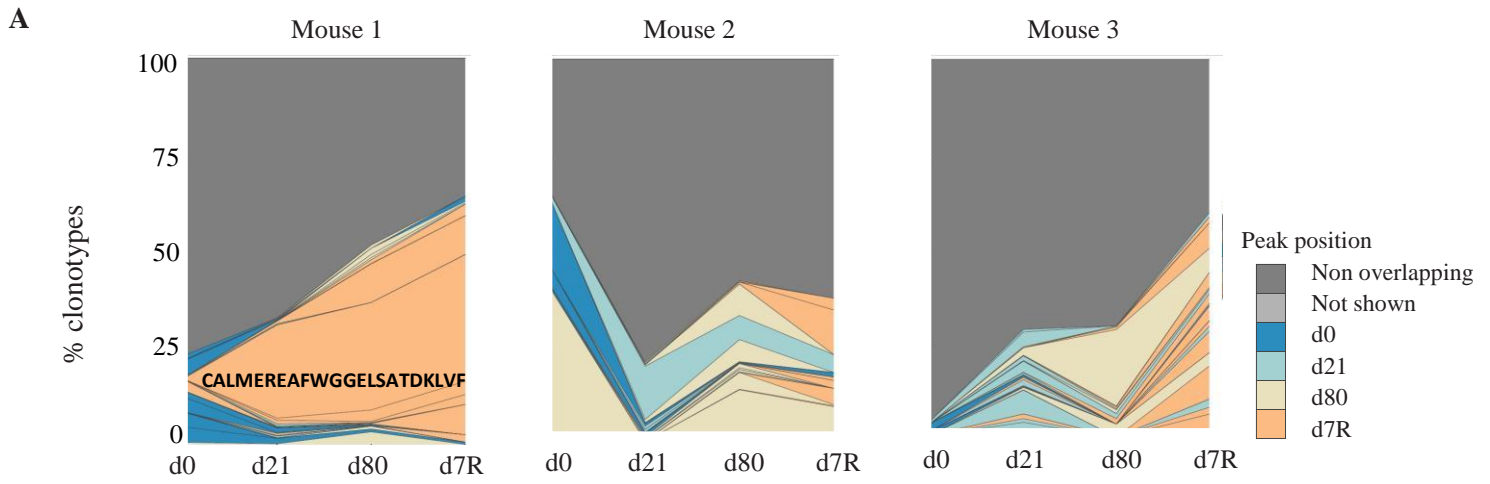
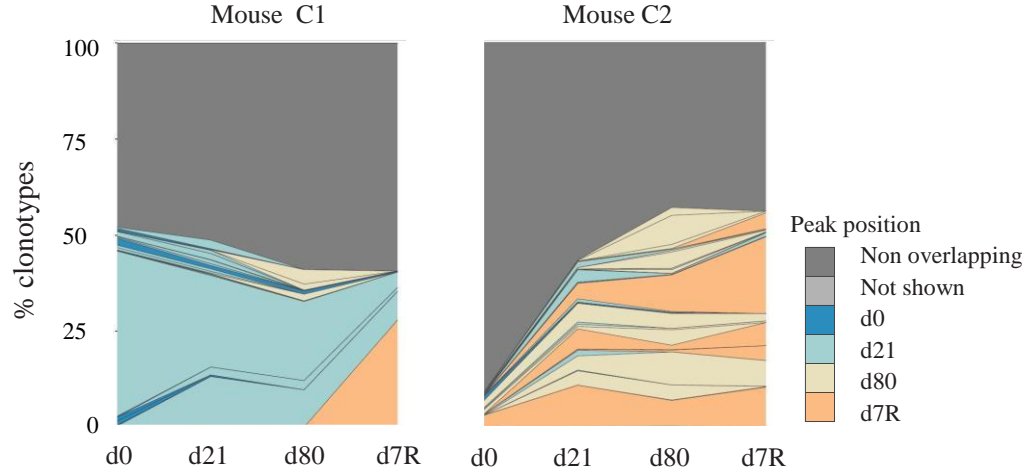


Fig 6

Infected Mice



Uninfected Mice



B Blood Organs

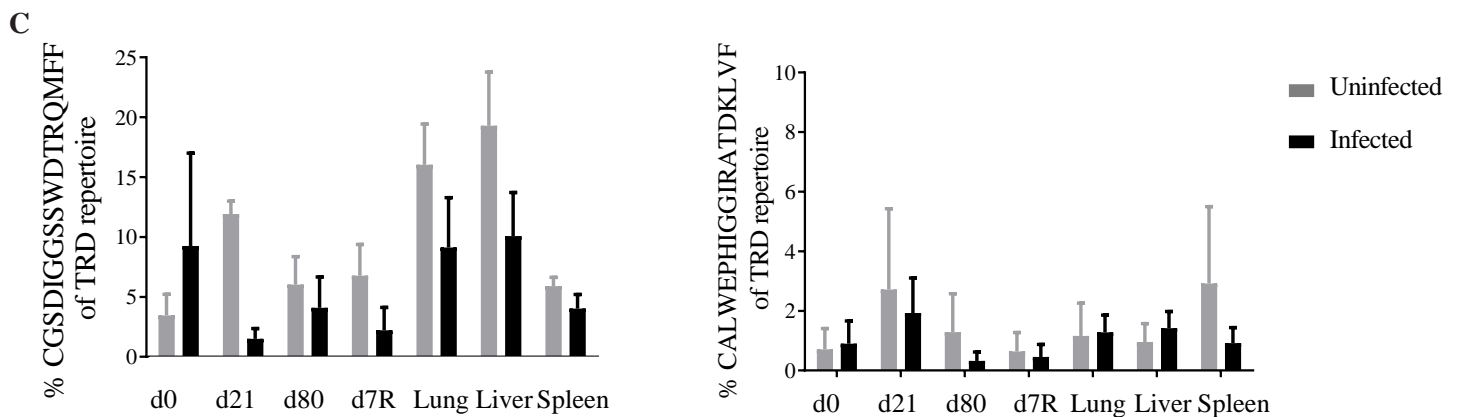
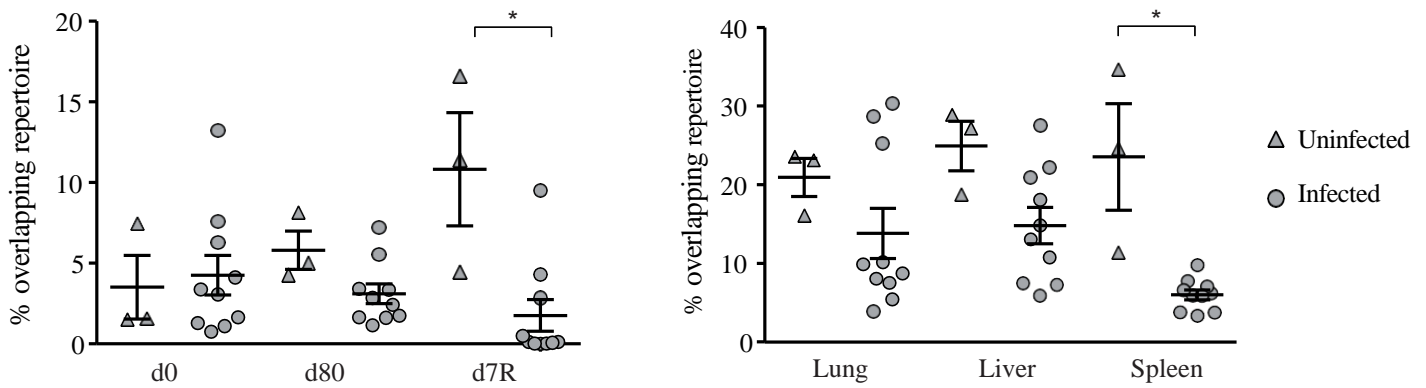


Fig 7

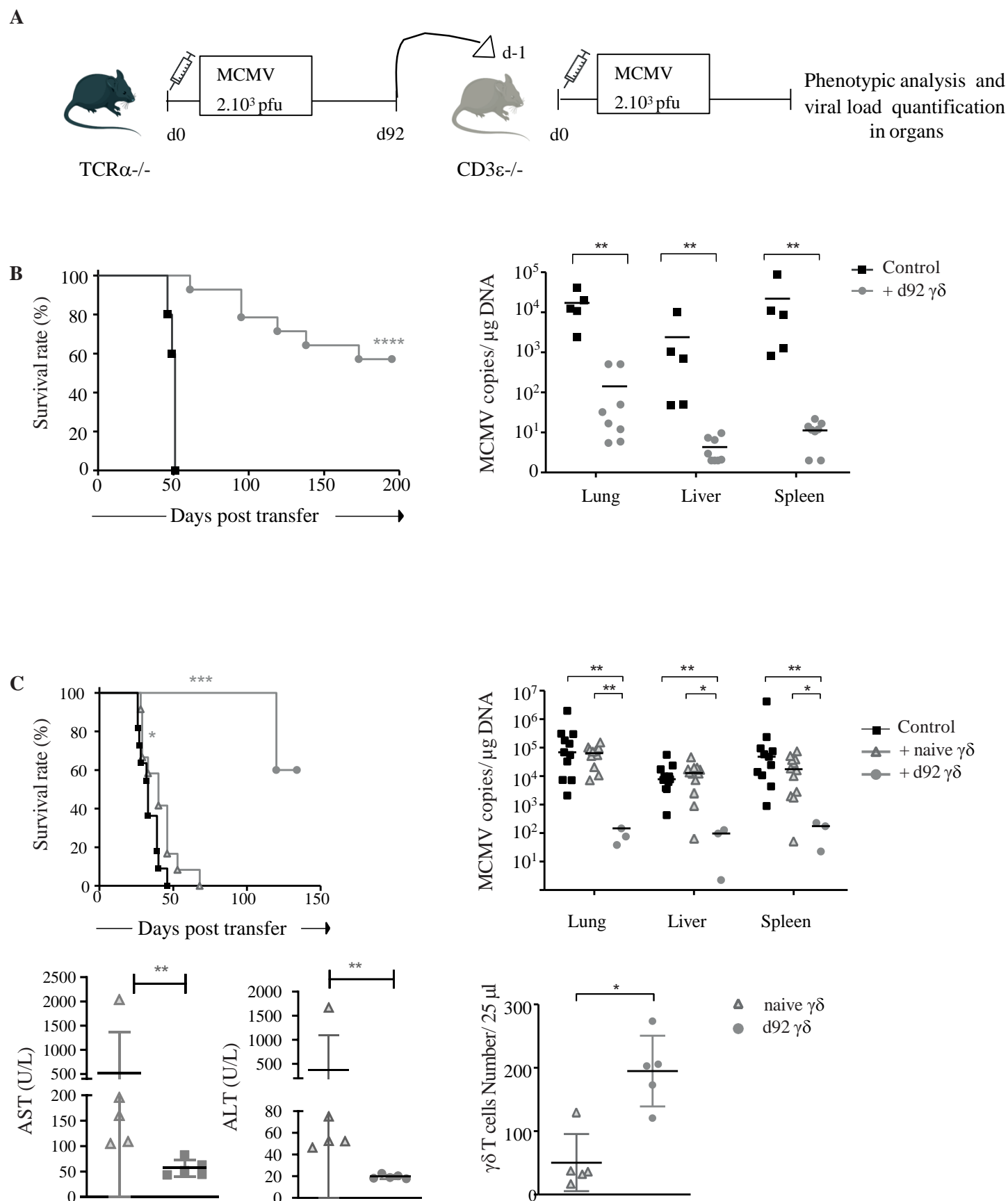


Fig 8

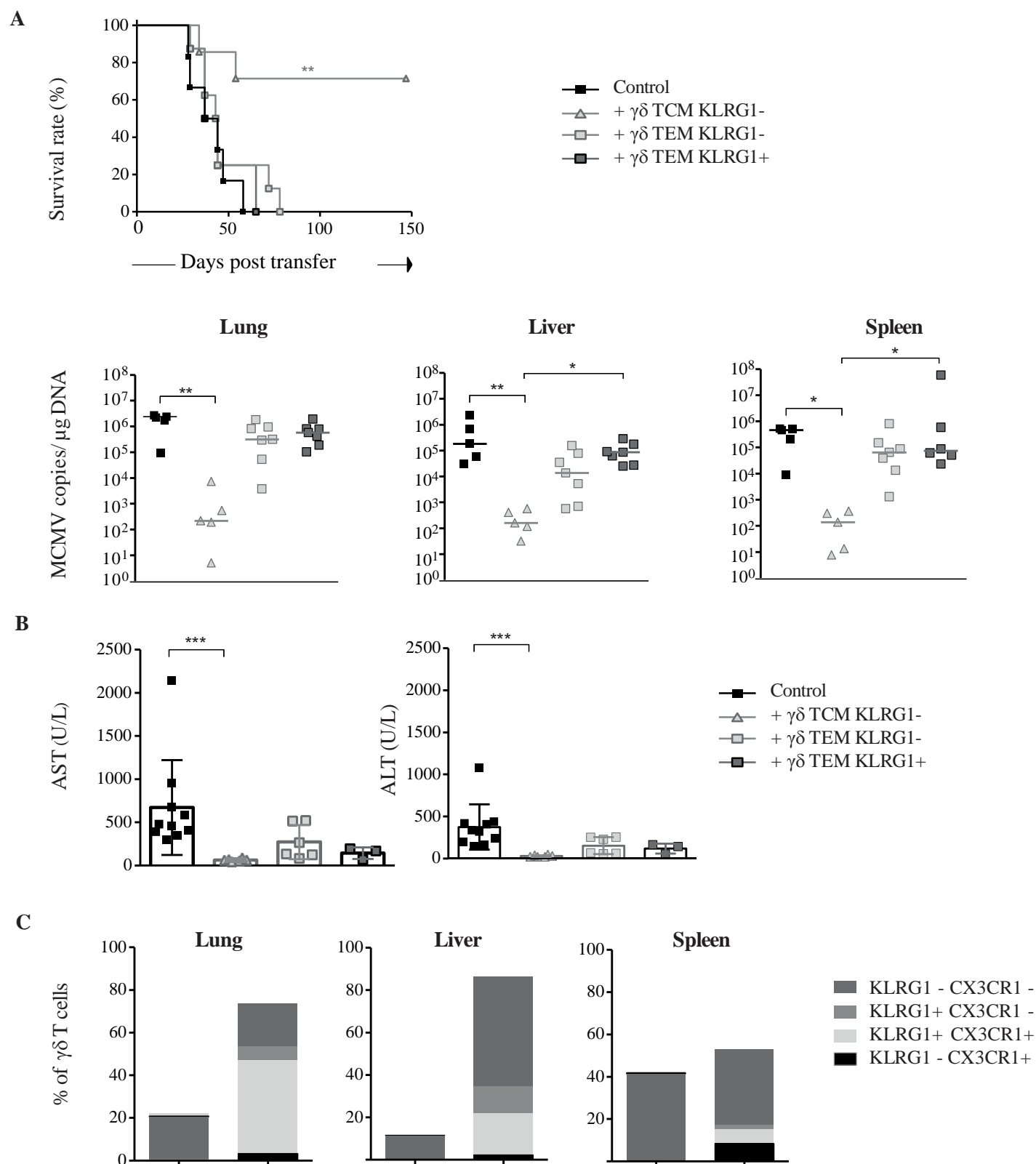
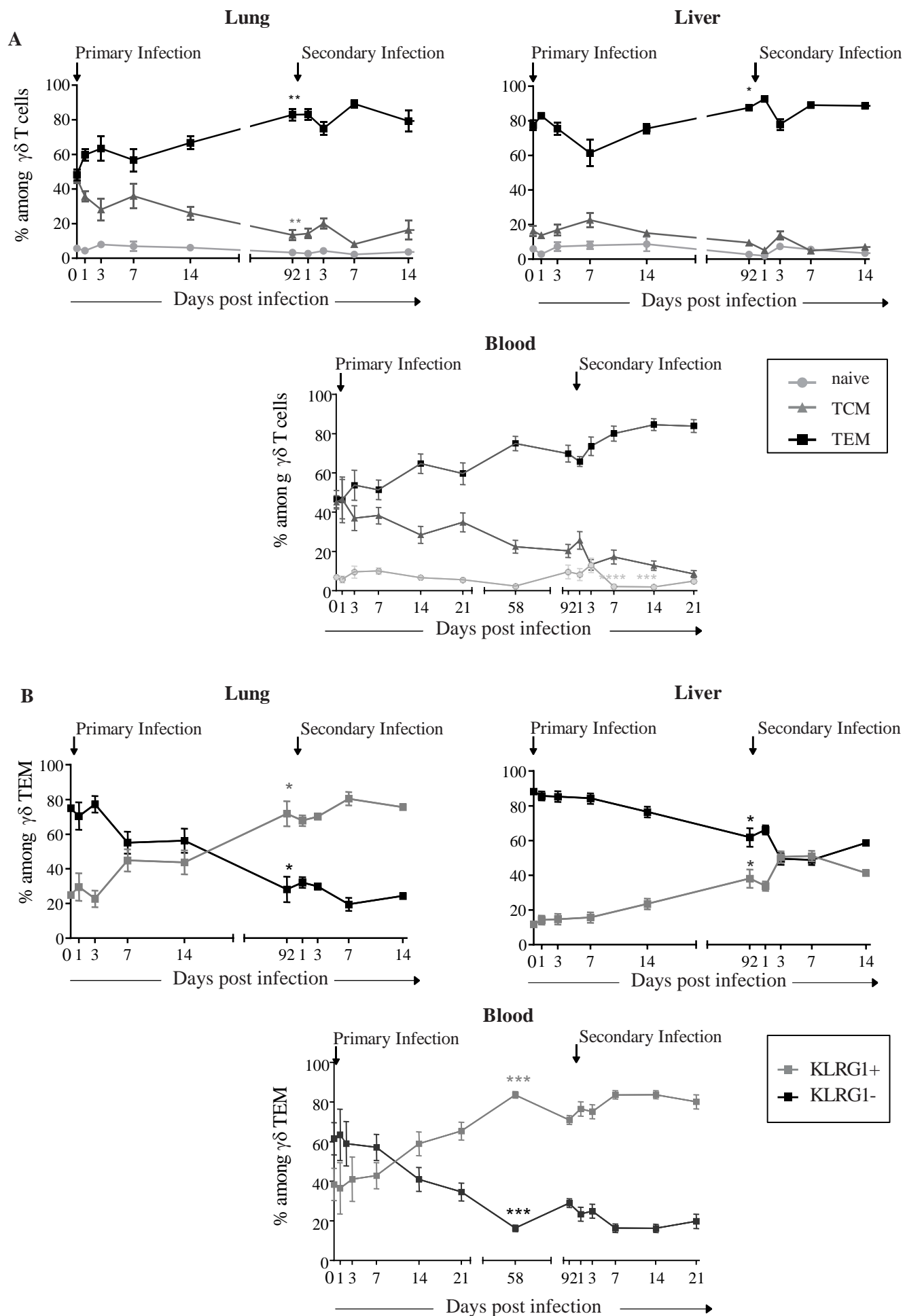
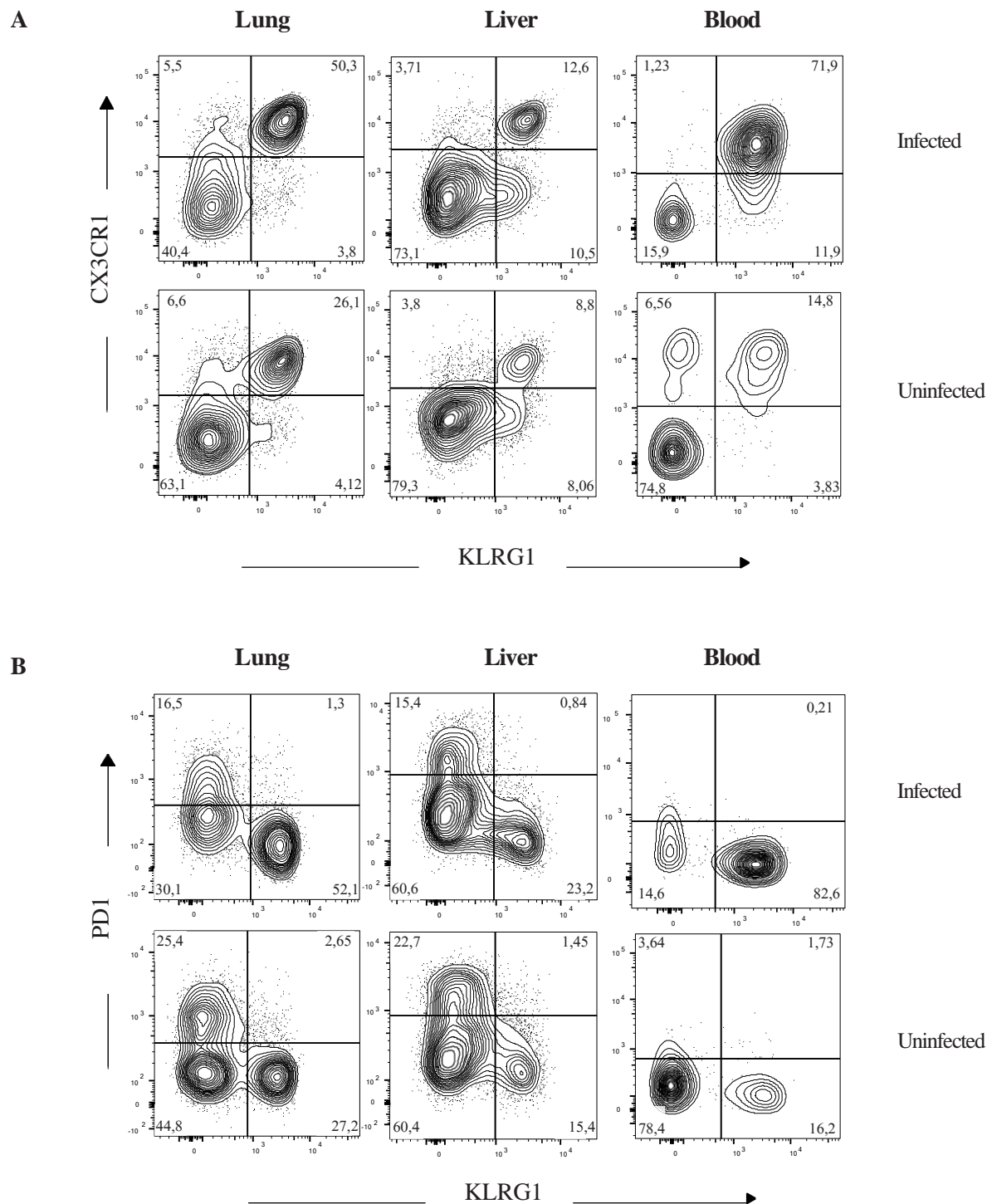
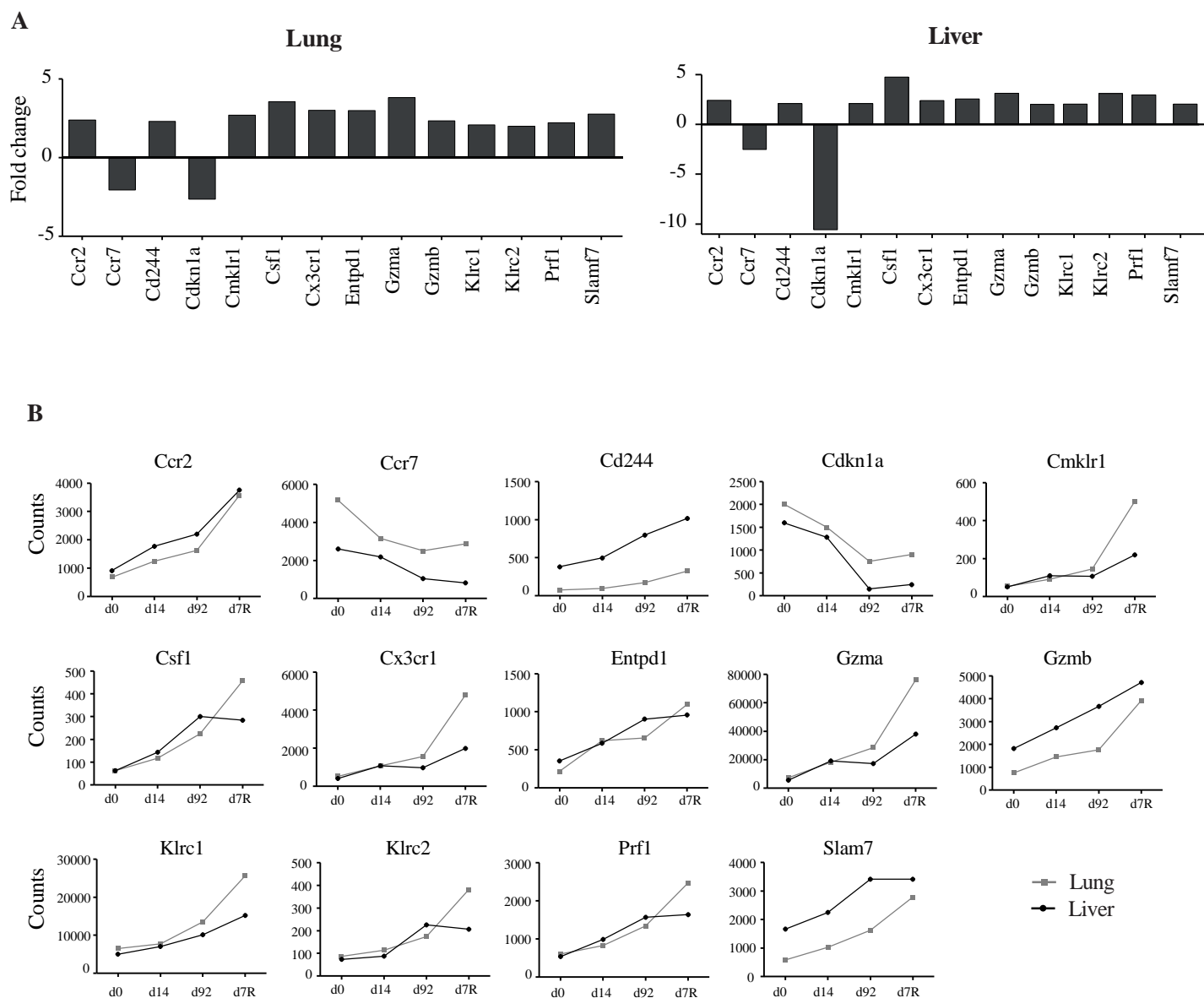


Fig 9

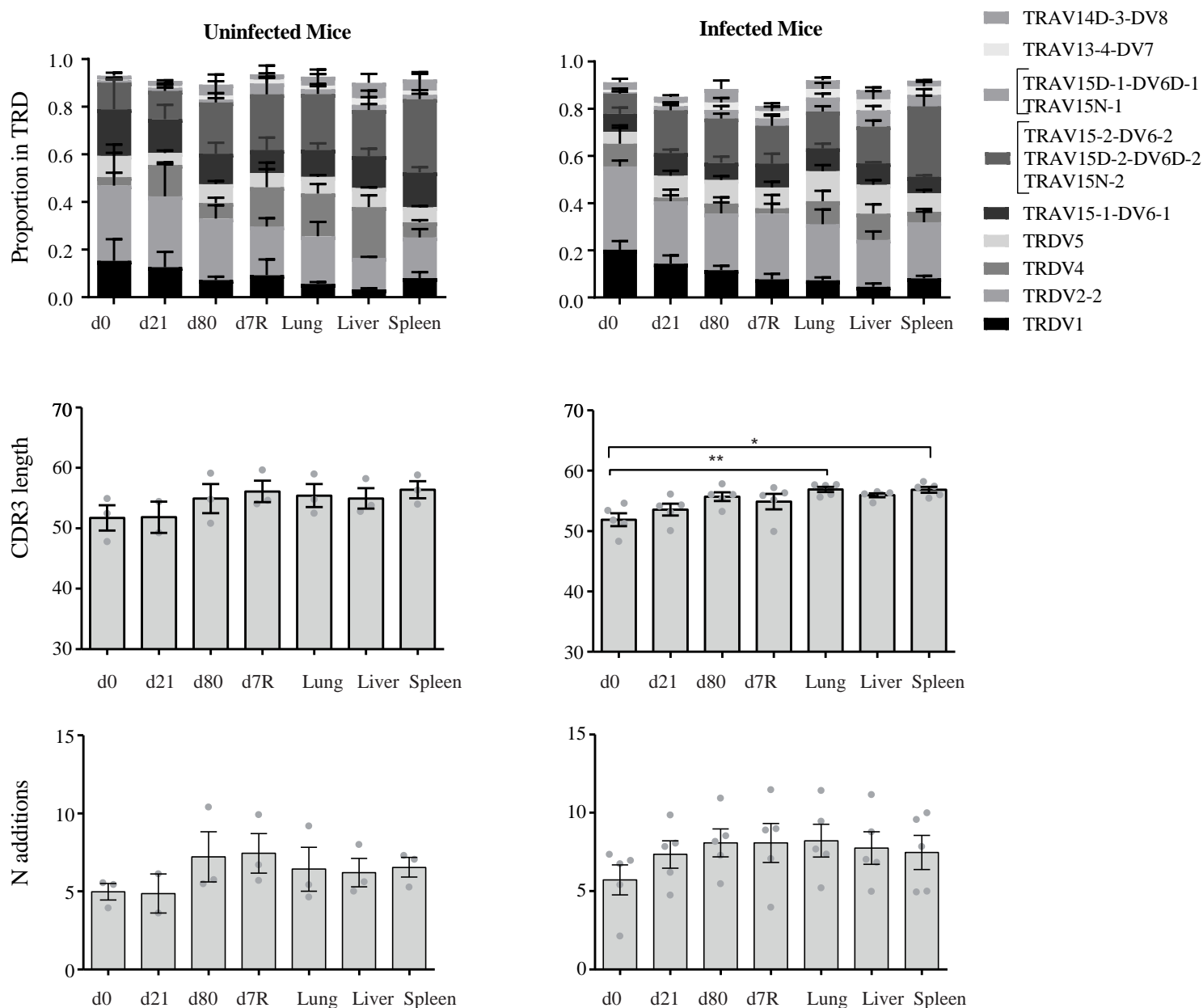


S1 Fig

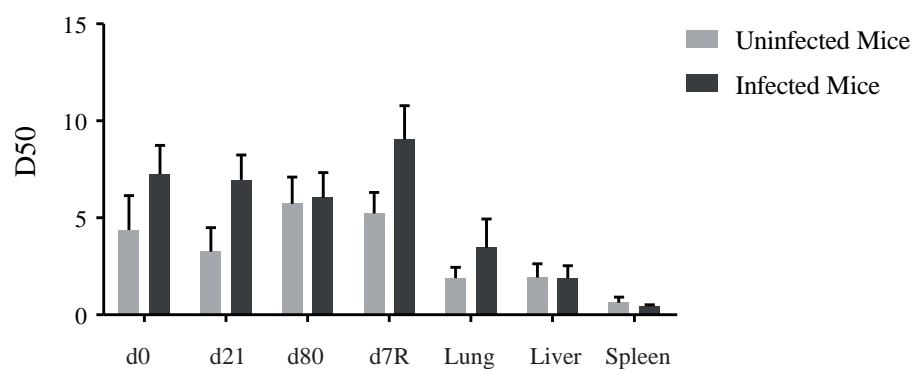


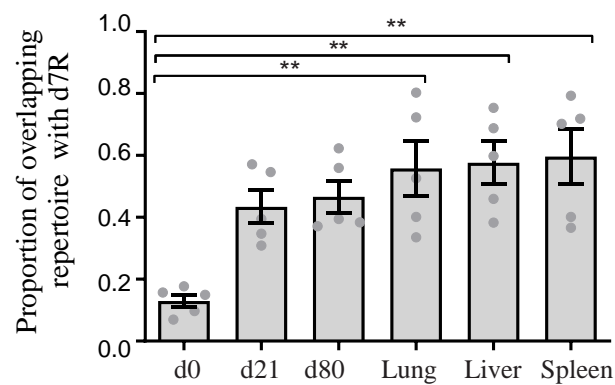
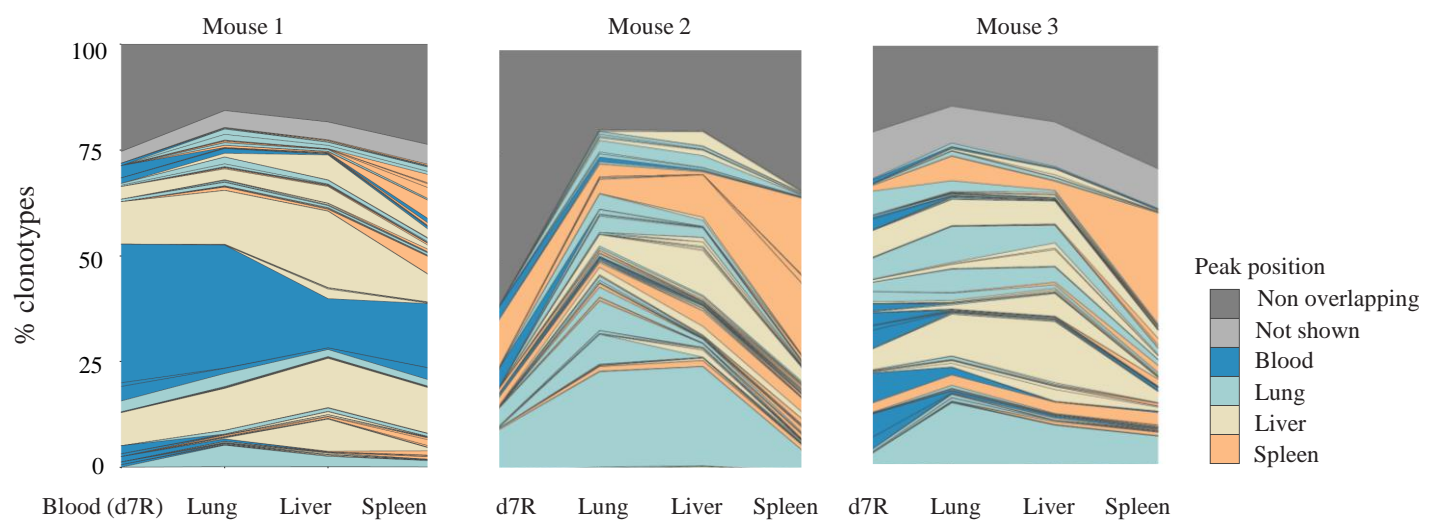


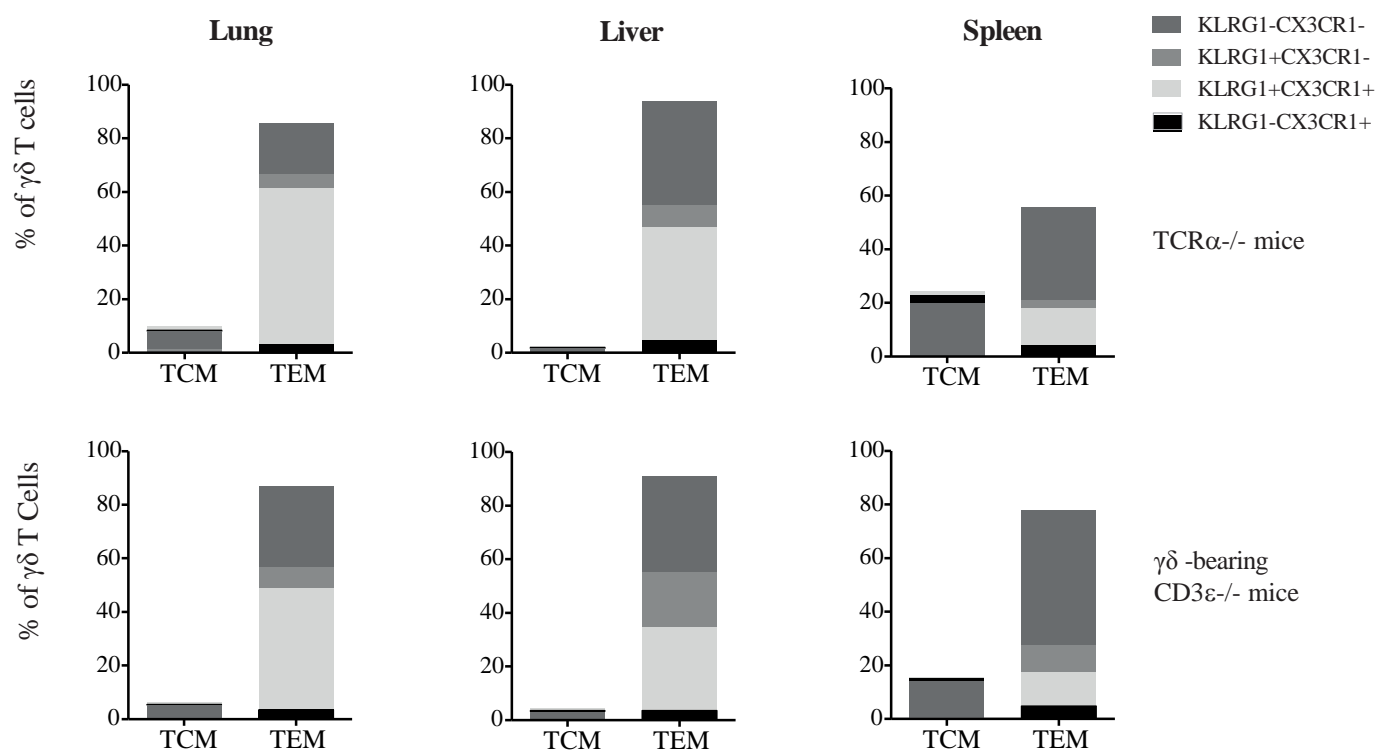
A



B







S6 Fig

